Modeling of liquid-vapor phase equilibria of pyrolysis bio-oils – a review

F.G. Fonseca [†]*, A. Funke*

Institute of Catalysis and Technology (IKFT), Karlsruhe Institute of Technology (KIT),
Hermann-von-Helmholtz-Platz 1, 76344 Eggenstein-Leopoldshafen

Abstract

The intricate composition of pyrolysis bio-oil necessitates the development of reliable phase equilibrium models, with a specific focus on liquid-vapor equilibrium pertinent to both condensation design and distillation, especially when utilizing non-wood feedstocks. Four key challenges intrinsic to pyrolysis bio-oil are scrutinized: the selection of an appropriate phase equilibrium model, formulation of a suitable surrogate mixture, representation of the elusive high-molecular-weight residue fraction, and the estimation of absent thermophysical properties. Despite a discernible inclination towards activity coefficient models, the literature reveals a diverse array of phase equilibrium models, pointing to the indispensability of considering a non-ideal liquid phase and raising concerns about the reliability of certain models in the absence of comprehensive experimental data. The judicious choice of a surrogate mixture emerges as pivotal, given the prevalence of unknown components and the dearth of precise compound-specific data, foreseeing a future where diverse surrogate mixtures coexist. Existing surrogate mixtures are reviewed and recommendations given to guide effective design of such mixtures. The absence of thermophysical properties for pyrolysis bio-oil compounds prompts the use of estimation methods, introducing a challenge in achieving comparable reliability to experimental values. Quantitative comparison of estimation performance shows no distinct trend favoring a singular estimation method, a composite of approaches is suggested to enhance overall model precision. To propel the field forward, a critical need is identified for augmented availability of reliable experimental phase equilibrium data for both pyrolysis bio-oil and its constituent compounds, coupled with their thermophysical properties, to establish a robust foundation for the widespread and efficient application of pyrolysis bio-oil across diverse industries.

Keywords: Fast pyrolysis; Condensation systems; Pyrolysis products; Thermophysical properties; Surrogate mixtures; Property methods; Separation techniques; Biofuels; Biochemicals; Biorefinery

Introduction

Despite increased investment and research into alternative energy sources, human daily activities still heavily depend on fossil fuels. Food, electricity, plastics, and chemicals production relies on petroleum, coal, or natural gas, and transportation mainly relies on petroleum-derived commodities. Petroleum accounts for a third of global primary energy consumption, followed by coal and natural gas [1]. This reliance has environmental, economic, and political consequences, including resource depletion and uneven distribution, as well as greenhouse gas emissions leading to climate change. To address this issue, humanity needs to transition from fossil fuels to other resources. Strategies include harnessing wind and water power, photovoltaic farms, and bioenergy from biomass. Bioenergy offers a reliable alternative with options for direct combustion for combined heat and power production or producing renewable alternatives for petroleum-based industries [2,3]. Using biobased waste materials is an increasingly important aspect to reduce environmental impcats, provide additional revenue streams, and address waste management problems [4].

Various techniques have been developed to produce liquid commodities from biogenic sources. Thermochemical conditions, including hydrothermal liquefaction, pyrolysis, and sub-stoichiometric combustion, offer advantages by eliminating the need for extraneous solvents. Hydrothermal liquefaction directly yields liquid phases, while pyrolysis and sub-stoichiometric combustion require condensation of reaction vapors [5,6]. The resulting liquids, termed bio-oil and wood vinegar, can serve as sources for fine chemicals or precursors for liquid transportation fuels [7]. Simultaneously, a solid carbon-rich char phase is produced, offering potential as a carbon source, method of carbon sequestration, solid fuel, or precursor for activated carbon production [8,9]. These versatile technologies support sustainable practices, replacing fossil fuels and reducing waste for a more environmentally friendly material and energy landscape. [3,10]

The design of the condensation system to recover liquids from pyrolysis plays a crucial role in the production of high-quality liquid products. The condensation process is responsible for cooling and condensing the vaporized pyrolysis products, resulting in a liquid bio-oil that can be used as biobased commodity. The design of the condensation system must take into account various factors such as the type of feedstock being processed, the desired product properties, and the operating conditions of the pyrolysis process. However, the design of efficient condensation systems, whether indirect or direct, is difficult to achieve using empirical or mechanistic models [11].

It has been observed that although reactors constitute a relatively small proportion of the total capital expenditure of a comprehensive system, the bulk of research and development efforts within the realm of fast pyrolysis have been directed toward optimizing reactor configurations and assessing feedstock suitability. Only in recent years has attention shifted towards optimizing overall process design, enhancing process control and improving condensation systems [12,13].

While carefully designed single stage condensation represents state of the art for commercial fast pyrolysis units, sequential condensation techniques are increasingly investigated and include condensers in series [14–16], multistage vapor quenching, cold traps at low temperatures [17], and manipulation of the sweeping flow rate inside the condensation vessels [18,19]. Such approaches allow for the production of multiple liquid streams of different compositions and characteristics. The operating conditions of each step are also tunable, optimizing characteristics for each liquid for further valorization [20]. For example, when employing sequencial condensation, a stream rich in water and light oxygenate organics may be produced. Due to its elevated water content, its value as fuel is negligible, but the high organic load inviabilizes cost-effective water treatment [21]. Nonetheless, strategies for its valorization have been studied, namely as a source of substrates for fermentation [21–23], a source of antimicrobian compounds [24], or can be mixed in to lower the viscosity or organic-rich condensates [14].

Single-stage bio-oils (BOs), and heavy fractions alike, feature a high-molecular-weight (HMW) fraction that accounts for a significant portion of its weight, and is comprised of a complex mixture of compounds with a wide range of chemical structures [25,26], which complete characterization is a challenging task, even when using combinations of analytical techniques [27–31]. One of the main challenges in characterizing this fraction is that it is frequently not volatile enough to be processed using gas chromatography (GC) [19,32–34]. This fraction is frequently associated with the water-insoluble fraction of BOs, and to the concept of ‘pyrolytic lignin’ [35]. However, there is not enough data available to evaluate to which extent this holds true. It is thought to be composed of by-products of lignin decomposition, substituted sugars, and polyaromatics [36]. Even though the exact composition of this phase is still not fully understood, it is known that it plays an important role in phase equilibria during condensation through interaction with other, more volatile species, namely water, and ignoring its presence can lower the accuracy of phase equilibria models designed to model fractionation of oils or predict composition of condensates [37].

Next to improving condensation design, distillation [5,38–40], liquid-liquid extraction [41–43], membrane separation [44–47], molecular distillation [48] and cold-water fractionation [24,49] are techniques that gather increasingly higher attention for the valorization of condensates, of which the latter is well-regarded as an environmentally safe alternative [49]. Their application requires a good grasp on the thermodynamic modeling of the system and access to required thermophysical properties. The successful implementation of these technologies could help to make bio-oils a more viable source of renewable energy and chemicals.

The design and optimization of condensation systems requires profound knowledge of liquid-vapour phase equilibria (LVE) for the mixture of compounds that is produced from biomass pyrolysis. Many models are available to describe LVE in general, primarily pushed by the complex optimization process of petroleum refineries. Even though the fundamental physical models are valid for all substances, there are specific challenges for the application to biomass-based pyrolysis vapors. Alike fossil crude oil they also represent a highly complex mixture with a substantial share of unknown compounds, but in contrast to them there is a high degree of oxygenated functionalities, resulting in many polar compounds. One of the main compounds present is water (both from original feedstock moisture and produced by pyrolysis reactions), but there are also significant fractions of organic acids, carbohydrates, aldehydes, ketones, furans, monolignols ((di-)methoxy-)phenols) and others [7,32,37,50]. Consequently, vapor- and liquid-phase association phenomena, like those observed for organic acids, alcohols and aldehydes, play an important role during phase equilibria and its presence should be accounted for when selecting thermodynamic models for modelling such phenomena. The definition of a suitable surrogate mixture is likely to continue being a decisive step in enabling LVE calculation for this complex matrix, and the issue that a significant fraction is unknown (and likely will remain unknown in practical applications) in fact demands for suitable surrogates to be defined [7,32,37].

Another important challenge arises from the fact that several of the most relevant components are molecules that have not yet been studied in detail, and important physical properties that are required for models are missing, even when heavily simplifying the complexity of FPBOs. Gani and O'Connell [51] point out that methods to predict physical properties play distinctive roles in process design: a service role, by providing a specified set of property values when requested, an advice role, by advising on the feasibility, and an integration role, by contributing directly to the strategy of solving a problem. Property methods combine thermodynamic modeling with component and mixture property estimation and are paramount in all phases of process engineering: synthesis, design, control, and analysis (energy, environmental impact, economy).

The aim of this review is to provide a comprehensive analysis of LVE modelling for pyrolysis bio-oils as fundamental pre-requisite for the design of any condensing (and distillation) system. It focusses on the main challenges that arise from dealing with this specific matrix, i.e. deciding on a phase equilibrium model to be applied and defining a suitable surrogate mixture to represent bio-oil in this thermodynamic model. Two additional aspects are covered that interact heavily with these two, namely the representation of the unknown oligomers in pyrolysis oil and the availability of thermophysical properties.

Phase-equilibrium models

Phase-equilibrium models are often the kern of a property method, since they constrain the properties and parameters required to properly describe and estimate the properties of a system. Apart from phase-equilibria, property methods often contain several other models, such as the variation of thermophysical properties of chemical species within the system with state conditions (x, T, P, μ, the estimation of mixture properties from the individual species', and phenomena like heat of mixing, solvation, hydrogen bonding, Van der Waals forces, the Poynting effect, Henry equation for light gases, etc…).

The decision of which of these to use during the modeling of a process is paramount for the correct modeling of the phenomena taking place. Carlson et al. [52] discussed the criteria for the selection of which phase-equilibrium models to use for simulation in general. In his article, he defined four factors to have in consideration: the nature of the properties of interest, the composition of the mixture, pressure and temperature range, and availability of parameters. The user would be required to know if the mixture under study was heavy on polar components, whether the mixture contained electrolytes, the pressure of operation, and the existence of interaction parameters (such as dimerization, and hexamerization). The author also discusses methods to estimate missing property parameters that the chosen property packages might require.

To represent the complexity of organic mixtures that constitute most pyrolysis oils, general recommendation would point to the use of activity-coefficient models, such as e.g. UNIFAC, UNIQUAC, Wilson, and NRTL. These are recommended for systems in the vein of pyrolysis vapor condensation systems often operate at medium to low temperatures (120 °C to ice traps), the presence of electrolytes is often disregarded, and the bio-oil is characterized as a strongly polar solution. [52] Despite this more general recommendation, many other approaches have been chosen and published in literature, covering a wide range of phase equilibria models (see Table 3). This requires a more fundamental summary of available phase equilibrium models for the purpose of this review, which will be addressed in the following. At the end of this chapter, an evaluation and summary of important aspects with regard to pyrolysis bio-oil is provided.

The general criterion for equilibrium is that the Gibbs energy (G) of a system reaches a minimum at certain operatory conditions (temperature (T), and pressure (P)), given by Eq. 1), in which μ_i stands for the chemical potential and v_i for the stoichiometric number for each species i. [53]

$$\sum_j \left(\frac{\partial G}{\partial n_i}\right)_{T,p,n_{i\neq j}} v_i = \sum_j \mu_i v_i = 0 \qquad 1)$$

The chemical potential can be estimated using Eq. 2), in which a_i is the activity of each species i. [53]

$$\mu_i = G_i^{\ominus} + RT\ln a_i \qquad 2)$$

The activity of a component is defined as the ratio between the fugacities (φ_i) in a phase and the standard state (φ_i^{Θ}, Eq. 3)). Said fugacities can be estimated using equations of state (EoS). [53]

$$a_i = \frac{\phi_i(p,T,x)}{\phi_i^{\ominus}(p,T)} \qquad 3)$$

Raoult's law states that the partial pressure of a component in an ideal gas mixture is equal to its contribution to the whole pressure. The concept of fugacity (f_i) can be used to extend this concept to real gases (Eq. 4), in which φ_i stands for the fugacity coefficient of component i, and y_i to the vapor fraction of i). [54]

$$f_i^V = \phi_i^V y_i P \qquad 4)$$

This can be generalized to any possible phase, therefore for liquid-vapor equilibrium (LVE), the relationship of phases can be described by Eq. 5).

$$\phi_i^V y_i = \phi_i^L x_i \qquad 5)$$

Fugacity coefficients are usually estimated using an equation of state but liquid-phase fugacities may also be a function of liquid activity coefficient methods. Even in the case of the ideal gas equation-of-state (EoS), in which the vapor phase is described by the ideal-gas equation, and the liquid-vapor equilibrium is described by Raoult-Dalton's law (which assumes that the system is composed of many randomly moving point particles that do not interact), the user is required to provide not only system parameters, like temperature, pressure, and volume (assuming steady-state), but also parameters specific to each species, like the vapor pressure of the component. More complex EoS and associate models often require the additional input of other parameters. It may be the case that such properties are missing for mixtures comprised of components that have not been experimentally characterized, which requires estimation of these missing properties.

Cubic equations of state

Cubic EoSs are a class of equations that can be used to model the behavior of fluids. They are called "cubic" because they can be written as a cubic function of the molar volume, for example, the Van der Waals equation, shown in Eq. 6), for which a and b are component-specific parameters estimated from critical point properties [55]. Cubic EoSs are popular because they are relatively simple to use and can provide accurate predictions for a wide range of fluids. [53]

$$\left(P + \frac{a}{{V_m}^2}\right)(V_m - b) = RT \qquad 6)$$

Subsequent EoSs are usually improved versions of the Van der Waals formula, focused on handling shortcomings at sub-/supercritical conditions or improving the modeling of liquid phase phenomena. A very industrially relevant derived EoS is the Redlich-Kwong EoS (RK) [56], which is not only widely used but also serves as the foundation for further improvements. Among these improvements, the following can be counted: Soave (SRK) [56], Peneloux [57] [58], Twu [59], Peng-Robinson (PR) [60], Cubic-plus-Associated [61,62] [63], Mathias-Copeman [64] and

Schwartzentruber-Renon-Watanasari [65]. All of these Redlich-Kwong modifications have attracted industrial and academic use alike, with SRK and PR attracting the most academic attention. Holderbaum and Gmehling [66] proposed a method (predictive SRK) combining SRK and the UNIFAC group contribution method to predict LVE at high pressures.

Cubic equations of state estimate the properties of a fluid assuming the presence of a single hypothetical component. Therefore, parameters a, b and α must be estimated using mixing rules similar to the ones presented in Eq. 7) , for which $x_{i,j}$ is the molar fractions of each component, $a_{i,j}$ and $b_{i,j}$ are the a and b coefficients for each component, and $k_{a,ij}$ is a parameter specific to the interaction [54]. Other mixing rules have been developed to account for systems with strong size, shape, and polarity asymmetries, namely the Boston-Matthias (BM) [67], Fischer-Gmehling [68], Huron-Vidal (HV) [69], Michaelsen (MHV Quadratic) [70], Wong-Sandler [71], and Kabadi Danner (KD) [72] rules. Vidal and Bogdanić [71] stress important shortcomings of EoSs employing these more advanced mixing rules, mainly on the prediction of properties on mixtures containing molecules of very different sizes, situations of partial liquid miscibility (spontaneous phase separation), or diluted associating species, and the prediction of liquid-liquid-vapor equilibria (LLVE), both of which are computationally demanding and require robust algorithms.

$$\begin{gathered} a = \sum_i \sum_j x_i x_j \left(a_i a_j\right)^{1/2} \left(1 - k_{a,ij}\right) \\ b = \sum_i \sum_j x_i x_j \left(\frac{b_i + b_j}{2}\right) \end{gathered} \tag{7)}$$

Virial equations of state

Virial equations of state arise from a rearrangement of the Van der Waals equation considering a coefficient that quantifies the deviations from an ideal case, the compressiblily factor Z. Virial equations are infinite expansions (Eq. 8)) of this rearrangement considering species-specific (virial) coefficients (B, C on Eq. 8)) that permit account for the interactions of successfully greater numbers of molecules. Several EoSs based on this principle have been developed, mostly for light petroleum systems, of which relevant examples are the Benedict-Webb-Rubin EoS [73], and subsequent improvements by Brulé et al. [74], and the Lee-Kesler EoS [75], and subsequent improvements by Plöcker et al. [76].

$$Z_m = \frac{PV_m}{RT} = 1 + \frac{BP}{RT} + \frac{CP}{RT^2} + \cdots \qquad 8)$$

While non-polar substances in the vapor phase behave almost ideally, polar substances can exhibit large deviations to ideality or even association. The latter can be expected in systems with hydrogen bonding, leading to dimers, for which acetic acid is a common example, while an important outlier is hydrogen fluoride which forms hexamers instead, but is rarely relevant during biomass processing. [54,77] Having defined the concept of fugacity (Eq. 4)), it is possible to define the equilibria of dimerization ($2A \rightleftharpoons A_2$) as Eq. 9) [54].

$$K = \frac{f_{A_2}}{f_A^2} = \frac{\phi_{A_2} y_{A_2}}{\phi_A^2 y_A^2} \qquad 9)$$

Prausnitz et al. [78] showed that acetic acid (20 °C, 1 bar) is dimerized at around 95% in the vapor phase. In the system benzene + propionic acid, Nothnagel et al. [79] (142 °C, 1 atm) showed that the effect of dimerization in the apparent fugacity of propionic acid is very apparent for vapor fractions over 0.2. These phenomena are unlikely to happen during condensation and further downstreaming of pyrolysis vapors.

Nothnagel et al. [79] studied binary gas-phase systems and considered three types of interactions: two non-polar molecules; one polar and one non-polar molecule, without further interactions; two molecular with interactions, such as hydrogen bonding or complex formation, regardless of polarity. The authors proposed strategies to estimate the second Virial coefficient (B on Eq. 8)) for all these cases, and provided parameter values for several common interactions. Hayden and O'Connell (HOC) [80] built upon the work of Nothnagel et al. [79] and proposed an algorithm manner to determin B based on the critical properties, the Parachor and the dipole moment of the molecule, as well as an association parameter; the authors propose values between 1-4.5 for this parameter, with higher values favoring the occurrence of vapor-phase association.

Statistical Associating Fluid Theory

The Statistical Associating Fluid Theory (SAFT) considers that fluid mixtures contain not only monomeric molecules but also clusters of molecules, including, but not limited to, hydrogen bonding, donor-acceptor clusters, polymers, or dimerization. As the properties of these clusters are usually different from the monomers, the bulk fluid properties are also different, which can be accounted for using statistical mechanics, namely the perturbation theory.

Wertheim [81–84] expanded the residual Helmholtz energy of a fluid into a series of integrals of molecular distribution functions and their association potential and simplified it to an expansion series which can be truncated at different points, depending on the level of rigor and number of parameters. Chapman et al. [85] employed this extension to mixtures of spheres and chain molecules as a sum of three terms representing contribution from different intermolecular forces: segment-segment interactions (a^{seg}), covalent chain-forming bonds (a^{chain}), and site-site specific interactions, such as hydrogen bonding (a^{assoc}), shown in Eq. 10).

$$a^{res} = a^{seg} + a^{chain} + a^{assoc} \qquad 10)$$

Gross and Sadowski [86–88] developed the Perturbed Chain SAFT (PC-SAFT) as a direct improvement of the SAFT EoS, based on some modifications of the expressions for the dispersion forces. The attractive term is also estimated as a sum of first- and second-order perturbation terms, whose coefficients are based on the thermodynamic properties of chain molecules.

Pereda et al. [53] described a variant method entitled Group Contribution with Association Equation of State (GCA-EoS), which makes use of a group contribution version of the association term of the original SAFT equation, as well as the Group Contribution Equation of State devised by Skjord-Jorgensen [89]. The authors discuss the methodologies to estimate the fugacity and the compression factor to be employed during liquid-vapor equilibria calculations, as well as the importance of simultaneously estimating attraction and association parcel parameters based on experimental data, for mixtures containing both self-associating groups (e.g., hydroxyl, acid) and obligate cross-associating groups (e.g., ketone, ester). The authors point out that using this model, modeling highly asymmetric systems at near- and supercritical conditions can be successfully done using a single set of parameters, but that the existent database is not as rich as those of more conventional models [53].

Activity coefficient methods

When discussing activity coefficient methods, the basic LVE (Eq. 5)) is reworked as Eq, 11), in which y_i stands for the vapor fraction of i, φ_i^V for the vapor phase fugacity coefficient, which can be obtained using an equation of state, P for the operating pressure, x_i for the liquid fraction of i, γ_i for the activity coefficient, and $f_i^{*,L}$ for the liquid phase reference fugacity. [54]

$$y_i \phi_i^V P = x_i \gamma_i f_i^{*,L} \qquad 11)$$

In ideal conditions, $\varphi_i^V = 1$, and $\gamma_i = 1$, which reduces to Raoult's law (Eq. 12), in which P_i* stands for the vapor pressure of i). [54]

$$y_i P = x_i P_i^* \qquad 12)$$

However, in non-ideal conditions, φ_i^V can be estimated using an EoS, and $f_i^{*,L}$ can be estimated based on Eq. 13), in which $\varphi_i^{*,V}$ stands for the fugacity coefficient of i at system temperature and vapor pressure (P_i*) and $\theta_i^{*,L}$ stands for the Poynting correction to the pressure (which is only relevant at high operating pressure). [54]

$$f_i^{*,L} = \phi_i^{*,V} P_i^* \theta_i^{*,L} \qquad 13)$$

For the case of multiple liquid phases, equilibria between the different phases can be estimated using a simple analogy to Eq. 11), using Eq. 14).

$$y_i \phi_i^V P = x_i^{L1} \gamma_i^{L1} = x_i^{L2} \gamma_i^{L2} \qquad 14)$$

While theoretical models have been developed for the estimation of the activity coefficient of electrolytes, non-electrolyte solutions must make use of correlative methods making use of species-specific and inter-species interaction parameters [78,90]. Among these, the simplest are the Margules [91] and Van Laar [92] methods, making use of two parameters each. The Hiranuma [93] and Wilson [94] methods make use of three interaction parameters. None of these is usable when modeling systems featuring liquid-liquid equilibrium, so Renon and Prausnitz [95] built upon the Wilson equation to propose the NRTL (Non-Random Two-Liquids) equation, which is applicable in systems that feature several miscible liquid phases. The UNIQUAC method (UNIversal QUAsiChemical) [96,97] has been derived from a first-order approximation of interacting molecule surfaces in statistical thermodynamics. The authors approach the interaction forces as a sum of combinatiorial and residual parts, of which the former attempts to describe the dominant entropy of mixing and is determined only by the composition of the mixture as well as pure-component molecular size and shape; the latter describes intermolecular forces that dictate the enthalpy of mixing and depends on intermolecular adjustable parameters. This method is of complex implementation, as apart from interaction parameters, the user is required to supliment species-specific parameters, related to the dimensions of a single molecule, as well as the coordination number of closely interacting molecules around a central one. It is possible to consider intermolecular association phenomena, such as hydrogen bonding, e.g., in the work of Anderson et al for water and minor alcohols [98]. Pyrolysis bio-oils commonly contain highly oxygenated compounds, meaning polar behavior in solution and most likely also an abundance of different functional groups on the individual components in the solution, leading to different degrees of association or reaction within the solution [99]. The UNIFAC method, developed by Fredenslund et al. [100,101] as a transposition of the UNIQUAC method, presents a major advantage for the description of complex mixtures for which experimental data is lacking, in that the description of the components of the solution is realized as a sum of contributor groups. The main difference between UNIFAC and UNIQUAC is the methodology to estimate the parameters; the former approaches the fluid as a solution of molecular moieties corresponding to the contribution groups, instead of requiring experimental parameters specific to the components or the binary interactions as is the case for the latter.

The corpus of interaction parameters has been maintained since its inception by a group entitled the UNIFAC Consortium (www.unifac.org). Several methods have been developed to estimate substance-specific and binary interaction parameters for several activity coefficient equations and equations of state, based on UNIFAC groups [54]. Several other variants of UNIFAC have been developed, and are discussed in further detail by Muzenda [102], and include Liquid-liquid UNIFAC [103], Ionic Liquid UNIFAC [104] , Lyngby-modified UNIFAC [105] [106], Dortmund-modified UNIFAC (UNIFAC-DMD) [107], and UNIFAC by the National Institute of Standards and Technology (NIST-UNIFAC) [108]. An extension proposed by Dahl and Michelsen [109] included non-condensable gases as possible groups in the UNIFAC database, allowing for proper modeling of gas-liquid systems, but this extension is not standard in the modified variants of UNIFAC [54].

Choosing the Right Thermodynamic Method

It is almost impossible to analyse the reasons behind the very different choices to approach phase equilibrium models of pyrolysis oils (compare Table 3), but it certainly clarifies the high uncertainty within the R&D community as to which model is suited best. When approaching this challenge for pyrolysis bio-oils, attentive users will be confronted with missing parameters sooner or later. Different input parameters are required to compute phase equilibrium models and their amount and type varies for the different approaches.

Table **1** summarizes the parameters required for each component in a mixture when employing various methods to model liquid-vapor equilibrium. It is important to note that this table focusses on LVE specific reuirements and that additional parameters, including enthalpies of formation, phase change, and reaction, as well as heat capacity, transport properties (density, viscosity, thermal conductivity, diffusion coefficients), and solubility parameters, may be necessary for accurate condenser and/ or process modeling.

The restriction in available parameters is different depending on the software package, and in cases where estimation methods are in place by default it might not be obvious at all to the user that there are such restrictions. These parameters are most reliable if based on dedicated experimental studies, which are costly and primarily available for compounds of sufficient commercial interest. Estimation of binary interaction parameters is done using equilibrium experimental data. It is important to vary the operating conditions to properly estimate these parameters, as the variation with temperature and pressure can be accounted for within the results. Van Ness et al. [110] elucidate the importance of consistency tests to the experimental data to evaluate the estimated binary parameters, and how more parameters do not necessarily result in a more correct estimation. The authors propose a series of consistency tests and methods for data reduction. Marcilla et al. [111] analyzed several literature publications in which NRTL parameters had been estimated for LLE cases and reported several inconsistencies related to the lack of physical significance of said parameters. Due to their relevance to phase equilibrium models in general, but also for further process related studies, estimation of fundamental thermophysical properties like critical point properties, acentric factor, vapor pressure, molar volume etc are discussed in more detail in a separate section further below. More model specific developments for bio-oil relevant compounds are subject to current R&D which is important to advance the field;

Table **2** presents some examples for the determination of component-specific and binary interaction parameters.

Table 1. Parameters required for each component in a mixture when using the different types of thermodynamic models. Adapted from: [54]

Parameter	Cubic EoS	Virial EoS	SAFT	Activity coefficient
Molecular weight	✓	✓	✓	✓
Critical point properties	✓	✓	✓	×
Acentric factor	✓	×	✓	✓
Vapor pressure	✓	✓	✓	✓
Molar volume	✓	✓	✓	✓
Self-interaction parameter	×	✓ [a]	✓	×
Binary interaction parameters	✓	✓ [b]	✓	✓
Non-randomness parameters	×	×	✓	×
Molecular volume and surface area	✓[c]	×	×	✓[d]

a: Nothnagel and HOC. For the latter, estimated based on the Parachor and the molecular dipole moment.
b: LKP method.
d: For methods making use of UNIFAC for the estimation of specific parameters.
c: UNIQUAC: entire molecule; UNIFAC: sum of contributions of the different groups.

A comprehensive analysis of phase equilibrium models that allows for a reliable conclusion of a preferred approach, or even a tendency, is yet missing. Fonseca et al. [112] performed a study using 28 different combinations of a vapor-phase and liquid-phase methods to estimate deviations in the prediction of the condensate mass flow as well as the water and guaiacol content. Four different fractioned condensations (simple flash distillation, atmospheric pressure) systems [19,113–115] from the literature were considered and surrogate mixtures were designed based on GC/MS data reported on each reference. The authors reported several problems when employing the Nothnagel or HOC methods due a to lack of available parameters (similar issues had been reported by Onarheim et al. [116]) as well as an underestimation of the liquid mass flow for all cases (more pronounced for Peng-Robinson and Redlich-Kwong variants). When analyzing the water content in the liquid phase, deviations were the highest for the same methods, except those using Wong-Sandler or MHV2 mixing rules. A similar trend can be observed for guaiacol.

While this example includes several interesting observations relevant for the field, it should also be emphasized that it is based on literature data from pyrolysis studies. It is unclear how close the applied condensation systems in these studies approach equilibrium. A conclusive study relies on high quality equilibrium data specifically for pyrolysis bio-oils, which is a challenge that is only being approached lately [37,117]. However, based on the nature of the different phase equilibrium models in conjunction with the specific challenges of pyrolysis bio-oil, some general tendencies can be concluded.

Table 2. Development of existent methods for surrogate mixtures of pyrolysis oils using experimental data. Adapted from [118].

Reference	Process	Vapor-phase Method	Liquid-phase Method	Development
Bharti et al. [119]	Liquid-liquid equilibria of hydroxyacetone-water mixtures	- [a]	NRTL and UNIQUAC	Binary interaction parameters for NRTL and UNIQUAC for acetol-water
Cesari et al. [120]	Phase equilibria of phenolics in water and ethanol	- [a]	NRTL	Binary interaction parameters for NRTL (6 different phenolics)
Ille et al. [121]	Multiphase modeling of FPBO	GCA	GCA	Association parameters for aromatic methoxyl and hydroxyl groups.
Li et al. [122]	Extraction of anisole and guaiacol using butyl acetate	SRK	NRTL, UNIQUAC, and Wilson	Binary interaction parameters for NRTL, UNIQUAC, and Wilson equations;

				Proposal of a new UNIFAC-DMD group: aromatic methoxyl.
Li et al. [123]	Extraction of guaiacol from model sugar stream using ionic liquids	-[a]	NRTL	Binary interaction parameters for NRTL for water-guaiacol
Prieto et al. [124]	Modeling of fuel blends	GCA	GCA	Parameters for ethers and ether-alkane mixtues.
Sánchez et al. [125]	Multiphase modeling of FPBO	GCA	GCA	Parameters for phenol ethers.
Shang et al. [126]	Extraction of lignols from pyrolysis bio-oil using cyclohexane	-[a]	NRTL, UNIQUAC, and Wilson	Binary interaction parameters for NRTL and UNIQUAC (cyclohexane + 4 solutes)
Stephan et al. [127]	Liquid-liquid equilibria of water + pyrolysis oil solutes	-[a]	NRTL and UNIQUAC	Binary interaction parameters for NRTL and UNIQUAC (9 solutes)

a: The system did not consider the presence of a vapor phase.

EoS methods (cubic, virial, SAFT) often assume the presence of ideal liquids, which makes them unviable for complex liquid condensations. However, variations of cubic EoS designed to account for non-ideal liquid have successfully been used during the modeling of such phemonema (e.g., PR-BM, see Table 3). Similarly, activity coefficient methods can be paired with different EoS methods to more correctly model the vapor-phase. This can easily be implemented in flowsheeting software, but has not been the standard in other types of models [37,128]. In conclusion, EoS approaches can only be recommended with a careful choice how to account for non-ideal liquids.

Despite the reliability of EoS methods when paired with liquid modeling variants, the overwhelming majority of liquid phase models reported in Table 3 are activity coefficient methods. Among these, NRTL and UNIQUAC methods present a large fraction due to the relatively large experimental database of species-specific and binary interaction parameters present for a large variety of mixtures (in

Table **2**, one can see some of the most recent developments specific to pyrolysis condensates). The potential for modeling liquid-liquid equilibrium should not be discarded, and further differentiates the potential of these methods when contrasted to EoS and the Wilson method. Pyrolysis condensates present a wide variety of compounds for which these parameters are missing, and UNIFAC variants were divised to address this problem. However, several important issues lay on the use of this method: 1. a simplification of the molecule leads to a loss of information, 2. there is no standardized method to divide the molecules into contributor groups, meaning that different users may come to different results based on the same mixture, and 3. not all possible binary combinations between groups have been experimentally determined (however, UNIFAC parameters for missing interactions can be estimated using *ab initio* methods [108,129]). Some moieties may be difficult to represent using the currently estimated groups, an example being the quinones present in the work by Manrique et al. [130]. The group contribution nature of UNIFAC allows for the estimation of binary interaction parameters for other activity coefficient models, like Wilson, NRTL, UNIQUAC and SRK variants [54]. It is important to note that the user should always assess the generated values and maintain awareness of potential inaccuracies, as the quality of the data and underlying assumptions might not necessarily align with physically consistent parameters.

Table 3. List of thermodynamic methods used during LVE modeling of biomass pyrolysis downstream bio-oil processing. Adapted from [118].

Reference	Process	Vapor-phase Method	Liquid-phase Method
Brigagão et al. [17]	Pyrolysis of corncob	PR	UNIQUAC [c]
Campos-Franzani et al. [132]	Liquid-liquid extraction of guaiacol from hydrocarbons	- [a]	NRTL
Cesari et al. [134]	LLE of phenolic components in water	- [a]	NRTL
Dutta et al. [135].	Fast Pyrolysis + *In Situ*/*Ex Situ* Vapor Upgrading	PR-BM	PR-BM
Feng et al. [137]	Fast Pyrolysis Bio-oil Surrogate	- [a]	SAFT
Fardhyanti et al. [139]	Liquid-liquid extraction of phenol from pyrolysis bio-oil (coconut shells and spent coffee)	- [a]	UNIFAC
Fonseca et al. [19]	Fast pyrolysis (wheat straw)	RK	UNIFAC
Fonseca [118]	Fast pyrolysis (wheat straw)	SRK-KD	SRK-KD
Gorensek et al. [142]	Lignocellulosic biomass pyrolysis	PR	PR
Gupta et al. [143]	Fast pyrolysis multistep condensation	Ideal gas	UNIQUAC
Gura [145]	Fast pyrolysis of lignin	RK	UNIFAC-DMD
Gustavsson and Nilsson [34]	Flash pyrolysis of forest residues for boiler	Ideal gas	Wilson [b]
Hammer et al. [148]	Fast Pyrolysis of equine waste for boiler	Ideal gas	NRTL
Humbird et al. [150]	Custom FP reactor for pyrolysis (softwood, corn stover, switchgrass)	PR-BM	PR-BM
Ille et al. [37]	Fast pyrolysis (wheat straw)	Ideal gas	UNIFAC-DMD
Ille et al. [37]	Fast pyrolysis (wheat straw)	GCA	GCA
Jasperson et al. [154]	LLE of model FPBO components	- [a]	UNIFAC-DMD
Kabir et al. [131]	Pyrolysis of municipal green waste	PR-BM	PR-BM
Kougioumtzis et al. [133]	Production of 5-HMF from cellulose	Ideal gas	NRTL
Krutof and Hawboldt [117]	Distillation curve modeling for FPBO	Ideal gas	UNIQUAC
Mohammed et al. [136]	Technoeconomic analysis of Napier grass pyrolysis and oil upgrading	Ideal gas	NRTL
Mohammed et al. [138]	Pyrolysis of Napier grass bagasse	Ideal gas	NRTL
Motta et al. [140]	Pyrolysis of different Brazilian biomasses	Ideal gas	NRTL
Neves [141]	Pyrolysis and hydrotreatment of sugarcane bagasse	SRK-BM	SRK-BM
Onarheim et al. [116]	Fast pyrolysis of pine wood and forest residue	Ideal gas	UNIQUAC [c]
Parku et al. [21]	Fast pyrolysis of *Miscanthus* and coffee grounds	Ideal gas	UNIFAC-DMD
Peters et al. [144]	Fast pyrolysis of lignocellulosics (pine, eucalyptus, poplar, wheat straw)	PR-BM	PR-BM
Shahbaz et al. [146]	Slow pyrolysis of cellulose, hemicellulose, and lignin	PR-BM	PR-BM
Shemfe et al. [147]	Fast-pyrolysis + hydroprocessing for electrical generation (pine wood)	Nothnagel EoS	UNIQUAC
Stephan et al. [149]	Ternary LLE equilibria of water, isopropyl acetate/toluene, and bio-oil surrogate	- [a]	UNIQUAC, NRTL
Wagh [151]	Fast pyrolysis of mallee wood	Nothnagel EoS	UNIQUAC [c]
Wang et al. [152]	High-pressure reactive distillation of bio-oil	- [a]	NRTL
Žilnik and Jazbinšek [153]	Solvation of fast pyrolysis oils	RK EoS	UNIFAC

a: The system did not consider the presence of a vapor phase.
b: The authors defined the bio-oil as a binary mixture of water and a non-water pseudo-component, for which Wilson binary parameters were determined.
c: Component-specific parameters estimated in the Aspen Properties™ software using the UNIFAC group contribution method.

Designing surrogate mixtures for pyrolysis condensates

Apart from the need to reduce complexity of the problem, the use of surrogate mixtures for pyrolysis bio-oils is required since several chemical compounds are simply unknown. This section will briefly introduce main chemical compounds in pyrolysis bio-oil to then review how these mixtures have been represented in literature. This is followed by a specific sub-section focusing on how to represent the unknown compounds in pyrolysis bio-oil.

Fast pyrolysis bio-oil (FPBO) is one example of a liquid product from pyrolysis, which is comparably well-studied and commercially marketed as industrial boiler fuel. It is a dark brown, free-flowing complex organic liquid composed of over 1000 organic compounds, and with a distinctive smoky odor attributed to the presence of guaiacols [155]. Its heating value is similar to the feedstock biomass (16-19 $\mathrm{MJ \cdot h^{-1}}$ [155,156]), and its water content between 15-50 wt.% [10,157], dependent on the feedstock moisture content, the presence of secondary pyrolysis, and condensation operating conditions [158]. Its low pH limits its long term storage potential and increases the cost of the equipment designed to handle it, but nonetheless it has found commercial use as boiler fuel and is currently being studied as a source of high-value chemicals [159], transportation fuels (after upgrading) [160,161], or for co-processing in conventional petro-refineries [162,163].

Solvent fractionation can split the FPBO into fractions of specific functionalities/ characteristics. E.g. in a first stage, FPBO can be divided into water-soluble and insoluble phases; in a second, each of these phases can be further characterized after extraction using dichloromethane (DCM) or diethyl ether (DEE) [164]. The use of acetone is disavowed due to degrading the structure of solids and macromolecules present in the condensate [165]. The water-insoluble phase makes up between 3-29 wt.%, and is commonly associated with low-molecular-weight (DCM-soluble) and high-molecular-weight lignin (DCM-insoluble), which is also referred to as 'pyrolytic lignin' [164]. The analysis of the bio-oil and its fractions is typically achieved using chromatography methods (GC/MS, GC/FID, HPLC), NMR, carboxylic number and total acid number [166,167], of which the standard is often the combination of GC/MS and GC/FID [168].

The most abundant products in the FPBO, except water, tend to be organic acids, aldehydes, and ketones. They are attributed to the ring scission of holocellulose but can also be end-chain products of other parallel decomposition networks [7,169–173]. The pyrolysis temperature leads to increased cracking reactions, resulting in an abundance of light volatiles, mainly ketones. Acetic acid, for example, is mainly derived from the elimination of an acetyl group linked to xylose but may be formed by the cracking of lignin side-chains or the decomposition of levoglucosan [172,174]. Organic acid species can also undergo dehydrogenation and decarboxylation to yield light alkanes, which enrich the gas phase and increase the yield of CO_2, or they follow esterification [7,175,176]. Trace amounts of aldehydes, esters, furans, and aromatics are also present, although aldehydes and furans are prone to instability and esters may form over time due to aging processes [7,177–183].

If rapid condensation methods are applied, relatively high yields of sugars are expected, which can be attributed to the transglycosylation of cellulose. The most abundant of these is levoglucosan, which may further convert into polyols, like glycols and butanediols [169,170,184]. Sugars are also known to undergo polymerization during pyrolysis, leading to the formation of char and CO_2. Furans, especially furfural, are expected to be obtained from the depolymerization of holocellulosic sugars. [7]

Typical lignin-derived compounds can be identified and are formed due to the cracking of the side-chains linking monomers together, forming volatiles as well as different high MW phenolics. Coumaryl units mostly yield phenol and alkyl-substituted phenols, such as vinyl-phenols and cresols. Guaiacyl units lead to methoxy phenols, such as guaiacol and substituted guaiacols, including eugenol and vanillin, being particularly common in the pyrolysis of softwood and contributing to the smoky odor of FPBO. Syringyl units degrade into dimethoxyphenols, such as syringol and substituted syringols. [7,168,178,185–190]

The behavior of FPBO is difficult to model using traditional methods due to above described complexity in composition. Moreover, there is a significant number of unknown compounds that are not detectable by commonly applied analytical methods and typically consist of oligomers that are abundantly formed during pyrolysis. One approach to overcoming this challenge is to use surrogate mixtures, which are simplified versions of the real product that contain only a few, representative key compounds [37,116,117,191].

The composition of a surrogate mixture depends on its intended purpose. If the goal is to model liquid-vapor equilibrium (LVE), then it becomes important to define a surrogate mixture for the pyrolysis process which corresponds to the boiling point range of the components which participate in liquid-vapor equilibria, of which some are reported in **Table 4**. Westerhof et al. [6,192] proposed a surrogate of 8 groups, corresponding to a range of 250 to 550 K to characterize condensates of pine wood pyrolysis. Ille et al. [37], Krutof and Humboldt [117], Adolf [191], and Onarheim et al. [116] defined surrogates based on reducing the complexity of GC/MS results (covering a boiling point range of 340-660 K). Jones et al. [193] modeled a system integrating fast pyrolysis and conventional upgrading technologies used in the petrochemical industry and therefore devised a surrogate based on several suggestions taken from the literature, based on typical groups present in biomass pyrolysis oils. Several of these mixtures are presented in **Table 4**.

It is very common for models to avoid issues with model representation by defining pseudo-components in which thermodynamic behavior is tuned to behave as intended or to simply select a simple surrogate mixture that simulates the special case under discussion. Such is the case of the model by Gustavsson et al. [34], in which the bio-oil is defined as a mixture of water and a non-water pseudo-component, for which Wilson EoS (equation of state) interaction parameters are defined to simulate experimental liquid-vapor equilibria. Another case is the study of Feng et al. [137], which described the bio-oil as a mixture of water and high market value sugar derivates to employ the statistical associating fluid theory (SAFT) EoS.

Wooley and Putsche [194] characterize a surrogate mixture suitable for wood processing in the pulp industry. The authors define a series of components based on their monomeric representation and estimate thermophysical parameters based on combustion data and the characteristics of plant-source materials. The complexity of the lignin phase is completely disregarded, as the latter is represented as a solid pseudo-component with little potential other than fuel. This perspective allows for a solid prediction of the heat availability of the system, based on using side streams as fuel. These results have been commonly applied in several publications, for example, the one by Peters et al. [144]. However, it was shown later that this high MW residue shows important interaction with other compounds in FPBO, such as e.g., water, thus influencing their behavior in phase equilibria [37,195]. It is required to adequately represent this residue with suitable surrogate compounds in consequence (see next section).

Another widely used application of pyrolysis bio-oil surrogate mixtures is for the modeling of pyrolysis reactions. They follow a very similar fundamental logic but are typically derived from a proposed, simplified reaction network and thus contain very different representatives. Several of these are presented in **Table 5** and **Table 6**. It is important to be aware of these differences, especially when it comes down to modelling a pyrolysis process. In that case, surrogate mixtures applied to the different process stages need to be aligned in one way or the other. Ideally, one surrogate mixture is used along the process; however, bearing in mind that these have to serve very different purposes (e.g., modeling chemical reactions vs LVE calculations) this is a challenging task.

From the review and discussion of surrogate mixtures found in literature, several additional considerations emerge for the design of a surrogate mixture:

- It is important to determine upfront the objective of the model because the surrogate mixture needs to include compounds and characteristics relevant for this objective.
- The analytical methods used to characterize the condensates and the vapors are very important. Chemometric methods like chromatography require databases and

calibrations for each different chemical species [7,19,162]. The absence of a component in the chemometric results of a complex mixture does not signify the absence of the component in the real mixture;

- Several chemometric methods do not distinguish isomers [196];
- Some chemometric methods, namely GC, feature temperature cutoffs (>280 °C [197,198]) above which a non-volatile component cannot be measured. For the case of pyrolysis oils, a significant proportion of high molecular weight compounds exist, some of which are related to the concept of 'pyrolytic lignin', that do interact with other molecules and thus effect phase equilibria. This effect needs to be included in the choice of a surrogate mixture, e.g. by adding representative(s) for these unknowns.
- Stability can be an important issue if the condensate(s) need to be transported or stored and strategies to mitigate this phenomenon include esterification, filtration, distillation or emulsification [181,199]. Due to a low pH and high number of reactive components, 'aging' is an important factor that must be taken into consideration when designing a surrogate mixture, as there can be a significant delay between obtaining the pyrolysis oil and its analysis [156,200];
- The properties of the surrogate mixture, such as density, vapor pressure or elemental composition, should be consistent with the properties of the real product.

The choice of surrogate mixture is an important decision that should be made carefully. It is likely that several different surrogate mixtures will coexist in future due to the nature of pyrolysis bio-oil and the different purposes these surrogates need to fulfil. A comprehensive analysis of the suitability of the different approaches is impossible to conduct given the current state of knowledge. Applied surrogate mixtures certainly provide guidance for applications, but more work is required to better elucidate this aspect of pyrolysis bio-oil phase equilibria modelling.

Table 4. Nominal bio-oil compositions (water-free) of surrogate mixtures used to model liquid-vapor equilibrium processes in the context of bio-oil separation. Values in brackets correspond to the boiling point at atmospheric pressure (ºC). Data taken from the PubChem database (https://pubchem.ncbi.nlm.nih.gov/) unless otherwise stated. Adapted from [118].

	Westerhof et al. [192]	**Westerhof et al. [6]**	**Ille et al. [37,201]**	**Krutof and Humboldt [117]**	**Adolf [191]**	**Jones et al. [193]**	**Onarheim et al. [116]**
Feedstock	Pinewood, three condensates	Pinewood, three condensates	Wheat straw, heavy (organic) condensate	Softwood shavings, single condensate	Wheat straw, light (aqueous) condensate	Pinewood sawdust	Pinewood / Forest residue
Acids	Formic acid (101), propionic acid (141), n-butyric acid (164)	Formic acid (101), acetic acid (118), propionic acid (141), n-butyric acid (164)	Acetic acid (118), propionic acid (141)	Acetic acid (118)	Acetic acid (118)	Crotonic acid (185)	Acetic acid (118)
Ketones			Acetol (147)	Acetol (147)	Acetol (147)	Acetol (147)	Acetol (147)
Alcohols	Ethanol (78)	Ethanol (78)	Ethylene glycol (197)	Methanol (65)	Methanol (65)		Ethylene glycol (197)
Aldehydes	Formaldehyde (-19), propionaldehyde (49)	Formaldehyde (-19)	Glycol aldehyde (131)	Glycol aldehyde (131)			Glycol aldehyde (131)
Furans			Furfural (162)	Furfural (162), Furfuryl alcohol (171)	Furfural (162)	Furfural (162)	Furfural (162)
Lignin derived	p-cresol (202), eugenol (254)	p-cresol (202), eugenol (254)	Phenol (182), Guaiacol (205), Syringol (261)	Guaiacol (205), 4-methylguaiacol (221), 4-ethylguaiacol (237), Eugenol (254), Syringol (261), 4-propylguaiacol (264), Vanillin (285)	Phenol (182)	Dimethoxybenzene (206), Isoeugenol (266), Vanillin (285), Dibenzofuran (287), Dimethoxystilbene (338)	Guaiacol (205)
Sugar derived	Hydroquinone (287)		Levoglucosan (385)**	Levoglucosan (385)**		Hydroquinone (286), Levoglucosan (385)**, Cellobiose (592)*	Levoglucosan (385)**
Extractives						Dehydroabietic acid (403)*	Oleic acid (360)
High MW residue		"pyrolytic lignin"	3,4,4'-bipheyltriol (389)*	3,4,4'-biphenyltriol (389)*		Phenylcoumarans (> 307), oligomeres with *β-O-4* bond	"pyrolignin"

*: Estimated using the Adapted Stein & Brown method by the US Environmental Protection Agency's EPISuite™.
**: Levoglucosan data obtained from Shoji et al. [202].

Table 5. Nominal bio-oil compositions (water-free) of surrogate mixtures used to model pyrolysis reactions. Values in brackets correspond to the boiling point at atmospheric pressure (ºC). Data taken from the PubChem database (https://pubchem.ncbi.nlm.nih.gov/) unless otherwise stated. Part 1 of 2. Adapted from [118].

Functional Group	**Ranzi et al.** [203 a]	**Corbetta et al.** [204]	**Anca-Couce et al.** [205]	**Peters et al.**[144 b]	**Trendewicz et al.** [206 c]	**Ranzi et al.** [207,208 d]	**Gorensek et al.** [142 e]
Alkanes			Methane (-162), ethylene (-104)	C1-C4 (-162 - -1), C5-C18 (36-316), cyclopentane (49), methylcyclopentane (72), cyclohexane (81), cyclohexene (83), methylcyclohexane (101), cyclopropylcyclohexane (156), n-propylcyclohexane (157), bicyclohexyl (238)			Methane (-162), ethylene (-104)
Acids	Acetic acid (118)	Acetic acid (118)	Acetic acid (118)	Formic acid (101), Acetic acid (118), Propionic acid (141), Levulinic acid (246)	Formic acid (101)	Acetic acid (118)	Formic acid (101), Acetic acid (118)
Acetons	Ketene (-56), Acetone (56), Diacetyl (88)	Acetone (56)	Acetone (56)	Ketene (-56), Acetone (56), Acetol (147)	Acetone (56)	Acetone (56)	
Alcohols	Methanol (65), Ethanol (78), iso-propanol (82), n-propanol (97), Ethylene glycol (197), 1,3-propanediol (214)	Methanol (65), ethanol (78)	Methanol (65), ethanol (78)	C1-C6,C9 (65-213), Ethylene glycol (197), Propanediol (214)	Methanol (65), ethanol (78)	Methanol (65), ethanol (78)	Methanol (65), ethanol (78)
Aldehydes	Formaldehyde (-19), Acetaldehyde (20), Glyoxal (50), Acrolein (52), Propanedial (122)*, 3-hydroxypropanal (149)*, hydroxyoxopropanal (183)*	Formaldehyde (-19), Acetaldehyde (20), Glyoxal (50)	Formaldehyde (-19), Acetaldehyde (20), Propanal (48), Propanedial (122)*, Glycol aldehyde (131)	Formaldehyde (-19), Acetaldehyde (20), Glyoxal (50), Propanedial (122)*, Glycol aldehyde (131)	Formaldehyde (-19), Acetaldehyde (20), Glycol aldehyde (131)	Formaldehyde (-19), Acetaldehyde (20), Glyoxal (50)	Formaldehyde (-19), Propanal (48), Glyoxal (50), Acrolein (52), Glycol aldehyde (131), 3-hydroxypropanal (149)*
Furans	Furan (32) THF (65) Furfural (162) HMF (270)**		HMF (270)**	Furan (32), Dimethylfuran (108)*, Furfural (162), Furfurylalcohol (171), HMF (270)**	HMF (270)**		Furfural (162), HMF (270)**

*: Estimated using the Adapted Stein & Brown method by the US Environmental Protection Agency's EPISuite™.
**: Estimated using the ACD/Labs Percepta Platform - PhysChem Module.
***: Levoglucosan data obtained from Shoji et al. [202].
a: Including secondary reactions reported in the Supplementary Information of the manuscript
b: Holocellulosic degradation taken from Ranzi et al. [203], lignin represented by a radicular degradation mechanism taken from Faravelli et al. [209]
c: Adapted from Corbetta et al. [204]
d: Both reaction networks feature the same pathways, with slightly distinct kinetic parameters
e: Adapted from Humbird et al. [150]

Table 6. Nominal bio-oil compositions (water-free) of surrogate mixtures used to model pyrolysis reactions. Values in brackets correspond to the boiling point at atmospheric pressure (ºC). Data taken from the PubChem database (https://pubchem.ncbi.nlm.nih.gov/) unless otherwise stated. Part 2 of 2. Adapted from [118].

Functional Group	**Ranzi et al.** [203] [a]	**Corbetta et al.** [204]	**Anca-Couce et al.** [205]	**Peters et al.**[144] [b]	**Trendewicz et al.** [206] [c]	**Ranzi et al.** [207,208] [d]	**Gorensek et al.** [142] [e]
Lignin derived	Phenol (182), Syringol (261), p-Coumary alcohol (297)*, Synapyl aldehyde (336)*	Phenol (182), p-Coumaryl alcohol (297)*, Synapyl aldehyde (336)*	Phenol (182), p-Coumaryl alcohol (297)*, Synapyl aldehyde (336)*	Benzene (80), Toluene (111), Ethylbenzene (136), Xylene (139), Phenol (182), p-Cresol (202), 2-ethylphenol (205), Guaiacol (205), Dimethylphenol (217), 4-isopropenylphenol (218), p-Coumaryl alcohol (297)*, Synapyl aldehyde (336)*, Synapyl alcohol (350)*	Phenol (182), p-Coumaryl alcohol (297)*, Synapyl aldehyde (336)*	Phenol (182), p-Coumaryl alcohol (297)*, Synapyl aldehyde (336)*	Anisole (154), Phenol (182), p-Coumaryl alcohol (297)*, Synapyl aldehyde (336)*
Sugar derived	Dihydrolevoglucosan (203)*, Xylose (328)*, Xylofuranose (331)*, Levoglucosan (385)***	Xylose (328)*, Levoglucosan (385)***	Xylose (328)*, Levoglucosan (385)***	Xylose (328)*, Levoglucosan (385)***, Glucose (411)	Levoglucosan (385)***	Xylose (328)*, Levoglucosan (385)***	Xylosan (247)*, Levoglucosan (385)***
Extractives						3,5-dihydroxy-benzofuranone (366)*, Gallocatechol (686)	3,5-dihydroxy-benzofuranone (366)*, Gallocatechol (686)
Polycyclics				Naphtalene (218), Chrysene (448)			
High MW residue						trans-3-(3,4-dimethoxyphenyl)-4-((E)-3,4-dimethoxystyryl)-cyclohex-1-ene (465)	trans-3-(3,4-dimethoxyphenyl)-4-((E)-3,4-dimethoxystyryl)-cyclohex-1-ene (465)

*: Estimated using the Adapted Stein & Brown method by the US Environmental Protection Agency's EPISuite™.
**: Estimated using the ACD/Labs Percepta Platform - PhysChem Module.
***: Levoglucosan data obtained from Shoji et al. [202.]
a: Including secondary reactions reported in the Supplementary Information of the manuscript
b: Holocellulosic degradation taken from Ranzi et al. [203], lignin represented by a radicular degradation mechanism taken from Faravelli et al. [209]
c: Adapted from Corbetta et al. [204]
d: Both reaction networks feature the same pathways, with slightly distinct kinetic parameters
e: Adapted from Humbird et al. [150]

Representation of the high-molecular-weight residue

This section discusses the challenges of accurately representing the HMW compounds in models of pyrolysis oil condensation. Different researchers have proposed various surrogates or representative molecules for this fraction, which is composed of complex, non-volatile compounds that are difficult to quantify experimentally. The choice of surrogate can significantly impact the accuracy of predictions made using these models, particularly when it comes to estimating the elemental composition of the bio-oil. Therefore, it is essential to carefully consider the selection of HMW surrogates and their limitations when developing and applying these models. It is also important to keep in mind that the presence, nature and abundance of the HMW residue is important to be able to make a mass and/or molar balance to the system.

There have been multiple approaches to better characterize the HMW residue. Elliott et al. [210] estimated the yield of water-insolubles as between 3-29 wt% (wet) of the FPBO yield, and estimate an average molecular weight of this phase as ranging between 1000-2500 g/mol. Czernik et al. [211] proposed values within the range 930- 980 g/mol for bio-oil after long term aging at different temperatures. Debiagi et al. [212] considered a surrogate 'high-molecular-weight lignin' with the formula $C_{24}H_{28}O_4$ (diethylstilbestrol dipropionate, 380.5 g/mol), as a subproduct of the degradation of lignin into sinapyl alcohol. A series of manuscripts concerning the characterization of the water-insoluble fraction of pyrolysis bio-oils [27,213–215] employ different characterization methods to a 'pyrolytic lignin' obtained by dropping pyrolysis oil from different sources into ice-cold water and then filtering and drying under vacuum. The authors characterized the obtained residue to have a molecular weight of 684-692 $g \cdot mol^{-1}$, an hydroxyphenyl / guaiacyl / syringyl (H/G/S, a common metric in the characterization of lignins) ratio of 6%/73%/21%, an elemental composition of 65.22% C, 6.13% H, and 27.63% O. They also found that the HMW residue contains 7.5% phenylic methoxy (CH_3–O–Ph) groups and 11.9% phenylic hydroxyl (OH–Ph) groups. Another molecular structure for the HMW residue has been proposed by Fonseca [37] based on the conclusions of Scholze et al. [213] (Figure 1). Bayerbach and Meier [215] reveal that there are additional substituents, such as acid (COOH–Ph, around 5% prevalence), acetyl (CH_3CO–Ph), resinol groups, and biphenyl bonds. The authors also propose a surrogate with the formula $C_8H_{7.18}O_{1.21}(OH)_{1.08}(OCH_3)_{0.37}$, with a molecular weight of 152.55 g·mol^{-1}.

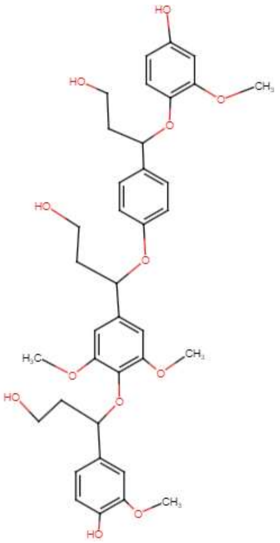

Figure 1. Molecular structure of an HMW residue surrogate based on the conclusions of Scholze et al. [213] ($C_{37}H_{44}O_{12}$, 680.74 g·mol^{-1}). Adapted from [118].

Other authors explicitly focus on representatives for the HMW residue phase that permit the modeling of LVE phenomena. Westerhof et al. [6] and Onarheim et al. [116] propose null vapor pressure surrogates with no specific identities (see Table 4), which at least enables its representation as mass fraction of the condensate. Ille et al. [37] [207] used low molecular weight dimer surrogates (Figure 2a and b) to model the HMW residue during simulations of LVE in pyrolysis condensates, with the intention to accurately model the activity of water. The decision for a suitable surrogate molecule was based on a systematic analysis of phenolic dimers using the UNIFAC-DMD model assuming ideal gas conditions and let to the recommendation of biphenyltriol (Figure 2b). Less accurate results were obtained by using a similar phenolic dimer (Figure 2c) during the modeling of fractional condensers using flash units and using the RK EoS [112].

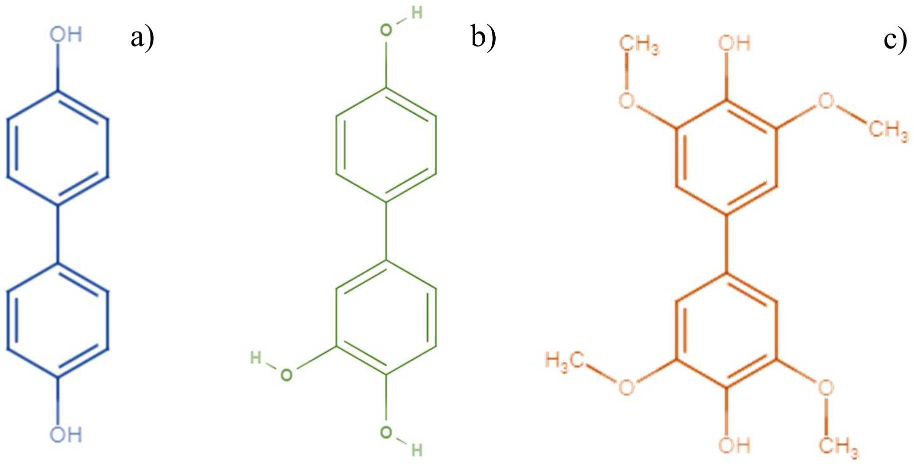

Figure 2. Molecular structure of a) 4,4’-biphenol ($C_{12}H_{10}O_2$, 186.21 g·mol); b) 3,4,4'-biphenyltriol ($C_{12}H_{10}O_3$, 202.2 g·mol^{-1}); and c) 4-(4-hydroxy-3-methoxyphenyl)-2,6-dimethoxyphenol, 276.28 g·mol^{-1}). Adapted from. [37,112,216].

Next to the accuracy of the phase equilibrium model, precise representation of the elemental composition of a bio-oil might be important. The amount of HMW residue and the choice for its representing molecule has an important influence on the elemental composition of the FPBO as can be seen in Table 8. For other modeling purposes, a more precise representation of the actual chemical nature of the HMW residue might be desirable. A ‘perfect’ solution for an HMW residue surrogate, in case it exists, has not been found and it is up to the user to decide on which alternative fits best the intended purpose of the study.

Table 7. Comparison of elemental composition (C/H/O, wt.% db.) between experimental and simulated pyrolysis condensates. Based on data taken from [118]. MC: moisture content.

	Wheat Straw MC = 1.2 wt.%	**Wheat Straw MC = 9.1 wt.%**	**Wheat Straw MC = 24.0 wt.%**	***Miscanthus***	**Sugar Cane Bagasse**	**Beech Wood**
Experimental	47.5%/6.7%/45.8%	54.6%/7.5%/37.9%	24.7%/3.5%/71.7%	43.7%/4.8%/51.4%	46.3%/5.9%/47.8%	42.3%/9.1%/48.6%
Simulated	59.8%/6.9%/33.3%	59.6%/6.9%/33.5%	59.7%/6.9%/33.3%	47.1%/11.1%/41.8%	59.1%/6.9%/34.0%	59.3%/6.9%/33.8%

Table 8. Nominal and fractional composition of several FPBOs in the literature, as well as an estimation of its elemental composition. Adapted from [37].

Ille et al. [37]				**Fonseca et al.** [19]				**Fonts et al.** [217]		
Composition	wt.%	mol.%		Composition	wt.%	mol.%		Composition	wt.%	mol.%
Water	13.3%	53.6%		Water	16.9%	47.4%		Water	23.2%	73.0%
Acetic Acid	5.1%	1.2%		Acetic Acid	14.6%	6.6%		Glycol aldehyde	1.0%	1.3%
Propionic Acid	1.3%	6.1%		Propionic Acid	3.7%	12.3%		Acetol	6.7%	5.1%
HAA	1.0%	1.3%		Acetaldehyde	2.6%	2.5%		2-Cyclopentenone	0.5%	0.3%
Acetol	9.0%	8.8%		Acetol	23.7%	3.0%		3-met-1,2-cyclopentedione	0.5%	0.3%
Furfural	1.6%	1.2%		Furfural	4.1%	16.2%		Acetic acid	8.7%	8.2%
Phenol	1.6%	1.2%		Phenol	4.0%	2.2%		Propionic acid	2.8%	2.1%
Guaiacol	2.7%	1.6%		Guaiacol	6.6%	2.2%		Formic acid	1.0%	1.2%
Syringol	2.4%	1.1%		Syringol	5.8%	2.7%		Furfural	0.6%	0.4%
Levoglucosan	3.7%	1.7%		Levoglucosan	9.9%	1.9%		2(5H)-furanone	0.8%	0.5%
Ethylene Glycol	1.4%	1.7%		Ethylene Glycol	8.1%	3.1%		Phenol	0.9%	0.5%
HMW residue [a]	57.1%	20.5%						Guaiacol	0.2%	0.1%
Elemental Analysis C/H/O	55.8%/6.5%/37.8%	34.7%/47.7%/17.6%		Elemental Analysis C/H/O	41.8%/8.0%/50.2%	24.0%/54.5%/21.6%		Creosol	0.5%	0.2%
								4-ethylguaiacol	0.2%	0.1%
								Catechol	0.3%	0.1%
								Syringol	0.1%	0.0%
								4-methylcatechol	0.5%	0.2%
								Vanillin	1.5%	0.6%
								Syringaldehyde	0.2%	0.1%
								Levoglucosan	6.5%	2.3%
								Cellobiosan	3.5%	0.6%
								HMM PL [c]	11.0%	0.4%
								LMM PL [d]	10.2%	1.0%
								Humin [e]	7.0%	0.6%
								Oligomer [f]	11.0%	0.4%
								Elemental Analysis C/H/O	42.6%/7.3%/50.1%	25.5%/52.0%/22.5%

a: 3,4,4'-bisphenoltriol ($C_{12}H_{10}O_3$, 202.22 g·mol^{-1}), b: $C_{37}H_{44}O_{12}$ (680.81 g·mol^{-1}), c: $C_{81}H_{78}O_{25}$, d: $C_{30}H_{34}O_{11}$, e: $C_{36}H_{32}O_{16}$, f: $C_{70}H_{82}O_{34}$

Estimation of thermophysical properties

The choice of a surrogate mixture should consider availability of experimental data for the thermophysical properties required to run phase equilibrium models; else these properties need to be estimated. Estimating thermophysical properties is an essential task in chemical engineering, particularly when dealing with complex systems where experimental data may not be readily available. Accurate estimates allow engineers to make informed decisions throughout different stages of a project, from process synthesis and design to optimization and control. Thermophysical properties influence the behavior of materials in various operations, such as separation, reaction, and heat transfer. Therefore, reliable predictions require careful consideration of the choice of phase equilibrium model, mixing rule, and thermophysical property estimation method in case reliable experimental data is missing. When modeling any system using phase equilibrium models other than Ideal Gas and unmodified Raoult law, the user is expected to supply properties such as critical point properties (temperature, pressure, volume, diameter, compression factor) for cubic and vapor-phase association equation-of-state methods (compare

Table **1**). Binary interaction parameters in both phases (calculated from experimental data, and available in several databases[1]) are required for several equation-of-state and activity coefficient models.

Table 9 and Table 11 show a list of experimentally-measured properties that are available in the literature and/or databases for typical pyrolysis condensate components. It is clear that the majority of parameters required to run phase equilibrium models for FPBO is missing. Of the compounds commonly used in surrogate mixtures, only acetic acid, p-cresol, methanol, and phenol have experimental values available for all parameters. Ethylene glycol, wich is a commonly used alcohol with higher normal boiling point than methanol, is also very well described. While lignin derived compounds sometimes have only be represented by p-cresol or phenol, it might by desirable and relevant to add other representatives (such as e.g. guaiacol and syringol) which are largely missing experimental data. It then needs to be decided whether to include them in a model, relying on estimating their thermophysical properties, or restrict the representation to the two compounds with more reliable data. One commonly used representative for furans (i.e. furfural) has larger gaps in experimentally determined parameters. Problematic are representatives for ketones (e.g. acetol), aldehydes (e.g. glycolaldehyde) and sugar derived compounds (levoglucosan) since experimental data for their thermophysical properties is largely missing. This shows that even for a surrogate mixture, which are typically created with the availability of thermophysical data in mind, significant gaps in experimental data to run phase equilibrium models do exist.

To overcome this challenge, it is required to rely on various methods to estimate physical properties, including Quantitative Property-Property Relationship (QPPR), Quantitative Structure-Property Relationship (QSPR) models, and *ab initio* models [217]. QPPR relates properties to one another through fundamental relationships, such as thermodynamic equations,

---

[1] It is possible to estimate binary interaction parameters using UNIFAC group contribution distributions for the NRTL, UNIQUAC, Wilson and Soave-RK models, and Huron-Vidal and Wong-Sandler EoS mixing rules.

or regression models. QSPR employs advanced molecular descriptors, including topological, topochemical, electrotopical, geometric, and hydrogen-bonding, along with computational techniques for optimization and regression. These methods enable the derivation of property values based on characteristics of the molecular structure. [218,219]. Among QSPR methods, group contribution methods are the most frequently used due to their ease of use and accuracy [220]. These methods divide the molecule into non-overlapping moieties, and the desired property is calculated as the sum of the properties of the molecular fragments, which are regressed from experimental data. Although this approach is straightforward, it does not consider isomerism. To address this limitation, second-order methods were developed, which take into account both the fragment itself and its nearest neighbors [221]. Typical group contribution methods permit the estimation of a property X following a formula similar to the one shown in Eq. 15), for which N_i and C_i and M_j and D_j correspond to the number of occurrences and contribution of a first-order group and second-order group, respectively.

$$f(X) = \sum_i N_i C_i + \sum_i M_j D_j \tag*{15)}$$

Table 9. Availability of measured thermophysical properties in the literature or databases for common biomass pyrolysis bio-oil components. Adapted from [118]. Part 1 of 2.

	Formula	CAS Number	Normal Boiling Point	Critical Parameters				Acentric Factor	Heat Capacity	Formation		Vapor Pressure	Enthalpy of Vaporization	Liquid Molar Volume
				Temperature	Pressure	Volume	Compression Factor			Enthalpy	Gibbs Energy			
Acetaldehyde	C_2H_4O	75-07-0	✓	✓	✓	✓	✓	✓	✓	✓	✓	✓	✓	✓
Acetic Acid	$C_2H_4O_2$	64-19-7	✓	✓	✓	✓	✓	✓	✓	✓	✓	✓	✓	✓
Acetol	$C_3H_6O_2$	116-09-6	✓							✓		✓		✓
Acetone	C_3H_6O	67-64-1	✓	✓	✓	✓		✓	✓	✓	✓	✓	✓	✓
Acrolein	C_3H_4O	107-02-8	✓							✓		✓		
Biphenyltriol, 3,4,4'-	$C_{12}H_{10}O_3$	3598-29-6												
Cellubiose	$C_{12}H_{22}O_{11}$	528-50-7	✓											
Crotonic acid	$C_4H_6O_2$	107-93-7	✓							✓				
Dehydroabietic acid	$C_{20}H_{28}O_2$	1740-19-8	✓											
Dibenzofuran	$C_{12}H_8O$	132-64-9	✓	✓	✓	✓			✓	✓		✓		
Dimethoxybenzene	$C_8H_{10}O_2$	202-045-3										✓		
Dimethoxystilbene	$C_{16}H_{16}O_2$													
Ethanol	C_2H_6O	64-17-5	✓	✓	✓	✓			✓	✓	✓	✓		✓
Ethylene Glycol	$C_2H_6O_2$	107-21-1	✓	✓	✓	✓		✓	✓	✓	✓	✓	✓	✓
Eugenol	$C_{10}H_{12}O_2$	97-53-0	✓										✓	
Formaldehyde	CH_2O	50-00-0	✓	✓	✓	✓	✓	✓	✓	✓	✓	✓	✓	✓
Formic Acid	CH_2O_2	64-18-6	✓	✓	✓	✓	✓	✓	✓	✓	✓	✓	✓	✓
Furfural	$C_5H_4O_2$	98-01-1	✓	✓					✓	✓		✓		✓
Furfural, 5-hydroxymethyl	$C_7H_8O_3$	67-47-0	✓						✓			✓		✓
Furfuryl Alcohol	$C_5H_6O_2$	98-00-0	✓	✓	✓					✓		✓	✓	
Glyoxal	$C_2H_2O_2$	107-22-2	✓									✓		
Guaiacol	$C_7H_8O_2$	90-05-1	✓						✓			✓		✓
Guaiacol, 4-ethyl	$C_9H_{12}O_2$	2785-89-9	✓									✓		
Guaiacol, 4-methyl	$C_8H_{10}O_2$	93-51-6	✓									✓	✓	✓
Guaiacol, 4-propyl	$C_{10}H_{14}O_2$	2785-87-7												

Table 10. Availability of measured thermophysical properties in the literature or databases for common biomass pyrolysis bio-oil components. Adapted from [118]. Part 2 of 2.

	Formula	**CAS Number**	**Normal Boiling Point**	**Critical Parameters**				**Acentric Factor**	**Heat Capacity**	**Formation**		**Vapor Pressure**	**Enthalpy of Vaporization**	**Liquid Molar Volume**
				Temperature	Pressure	Volume	Compression Factor			Enthalpy	Gibbs Energy			
Glycol Aldehyde	$C_2H_4O_2$	141-46-8										✓	✓	
Hydroquinone	$C_6H_6O_2$	123-31-9	✓						✓	✓		✓	✓	
Isoeugenol	$C_{10}H_{12}O_2$	227-678-2	✓									✓		
Levoglucosan	$C_6H_{10}O_5$	498-07-7	✓							✓		✓		
Linoleic Acid	$C_{18}H_{32}O_2$	60-33-3	✓	✓	✓			✓						
Methanol	CH_4O	67-56-1	✓	✓	✓	✓	✓	✓	✓	✓	✓	✓	✓	✓
n-Butyric Acid	$C_4H_8O_2$	107-92-6	✓	✓	✓	✓	✓	✓	✓	✓	✓	✓	✓	✓
Oleic Acid	$C_{18}H_{17}O_2$	112-80-1										✓		
p-Coumaryl Alcohol	$C_9H_{10}O_2$	3690-05-9	✓											
p-Cresol	C_7H_8O	106-44-5	✓	✓	✓	✓	✓	✓	✓	✓	✓	✓	✓	✓
Phenol	C_6H_6O	108-95-2		✓	✓	✓	✓	✓		✓	✓	✓	✓	✓
Propanaldehyde, 1-	C_3H_6O	123-38-6	✓	✓	✓	✓		✓	✓	✓		✓	✓	✓
Propionic Acid	$C_3H_6O_2$	79-09-4	✓	✓	✓	✓	✓	✓	✓	✓		✓	✓	✓
Sinapaldehyde	$C_{11}H_{12}O_4$	4206-58-0												
Syringol	$C_8H_{10}O_3$	91-10-1	✓							✓		✓	✓	✓
Vanillin	$C_8H_8O_3$	121-33-5	✓							✓	✓	✓	✓	
Xylosan	$C_5H_8O_4$	51246-91-4												

Another option is *ab initio* models, also referred to as quantum chemistry composite methods. These models simulate the behavior of molecules in a quantum space, allowing for the manipulation of interactions and conditions [222]. Researchers have attempted to combine machine learning with ab initio methods to estimate properties based on molecular structures [223], or predict the molecular structure of a hypothetical compound based on a desired property [222]. Additionally, combining QSPR and *ab initio* methods creates comprehensive databases for machine learning models [224]. Many software packages, such as e.g. Gaussian, provide access to pre-compiled model chemistry databases for these methods. Simmie and Somers [225] discuss the most commonly databases used for property estimation, and discuss issues arisen from the inexperienced use of these methods, as well as mentioning the need to develop model chemistries which are both resource-non-intensive, friendly to use, and employ more recent and better functionals.

In Table 11, one can find a list of methods to estimate relevant thermophysical properties. As most of them have more than one method available, it is the responsibility of the user to ensure the physical viability of the results obtained [226]. Gorensek et al. [122] devised alternative group-contribution-based strategies to estimate several of properties for both solid and liquid compounds. Several of the methods presented in Table 11 are correlation methods in function of process conditions, such as temperature and pressure. This allows for a better estimation of process conditions and product quality during different phases of a chemical engineering project (process synthesis, design, optimization, control and analysis). [227] Consequently, the variation of the properties with the state conditions (P, T, V, n, μ) have to be made available for each participating component, in each individual phase-equilibrium calculation.

Rowley et al. [228] affirms that thermophysical property databases frequently do not perform consistency checks on the results contained within, and propose 39 diffferent possible checks, including estimation of the critical compression factor from the definition vs from the other critical properties, testing whether the parameters fit within a certain range, or even comparing the value estimated for the vapor pressure between solid and liquid at the melting temperature. These tests can be automatized within the database to single out faulty data, signifying unfeasible experimental results or unsuitable estimation parameters.

Table 11. List of methods for estimation or correlation of relevant thermophysical properties. Not extensive. Adapted from [118].

Parameter	Group contribution methods	Other QSPR methods
Normal Boiling Point	Joback [229], Gani [230], Cordes-Rarey [231], Satou [232], Stein-Brown [233], Marrero-Gani [234], Marrero-Pardillo [235]	Mani [a], Twu [236]
Critical Temperature	Joback [229], Gani [230], Lydersen [237], Fedors [238], Ambrose [239], Klincewicz-Reid [240], Nannoolal-Rarey [241], Marrero-Gani [234], Marrero-Pardillo [235]	Mani [a], Twu [236]
Critical Pressure	Joback [229], Gani [230], Lydersen [237], Ambrose [239], Nannoolal-Rarey [241], Marrero-Gani [234], Marrero-Pardillo [235]	Mani [a], Twu [236]
Critical Volume	Joback [229], Gani [230], Lydersen [237], Ambrose [239], Fedors [242], Nannoolal-Rarey [241], Marrero-Gani [234], Marrero-Pardillo [235]	Twu [236]
Acentric Factor		Lee-Kesler [243]
Ideal Gas Heat Capacity	Benson [221], Joback [229], Harrison [244]	Aly-Lee [245]
Liquid Heat Capacity	Růžička [246–248], Chueh-Swanson [249]	
Standard Enthalpy of Formation	Joback [229], Gani [230], Benson [221] Marrero-Gani [234]	
Standard Gibbs Energy of Formation	Joback [229], Gani [230], Benson [221] Marrero-Gani [234]	

Vapor Pressure	Li-Ma [250], Nannoolal-Rarey [251], Simmons [252], Yair-Fredenslund [253], Ceriani-Meirelles [254]	Mani [a], Riedel [255], Mackay [256], Mishra-Yalkowsky [257], Myrdal-Yalkowsky [258]
Enthalpy of Vaporization	Gani [230], Vetere [259,260], Ducros [261–263], Li-Ma [250], [257], Marrero-Gani [234]	Watson [264]
Liquid Molar Volume	Le Bas [265]	Gunn-Yamada [266], Yamada-Gunn [267], Rackett-Spencer-Danner [268], Hankinson-Thomson [269,270], Honarmand [271]
Vapor Viscosity	Reichenberg [272]	Chung-Lee-Starling [273]
Liquid Viscosity	Letsou-Stiel [274], Orrick-Erbar [275], Nannoolal-Rarey [276]	
Vapor Thermal Conductivity		Chung-Lee-Starling [273]
Liquid Thermal Conductivity	Sastri-Rao [277], Navgekar-Daubert [278]	Scheffy-Johnson [279], Sato-Riedel [275], Lakshmi-Prasad [280], Gharagheizi [281]
Surface Tension	Li-Ma [250]	Brock-Bird [282], MacLeod-Sudgen [283,284], Zuo-Stenby [285], Sastri-Rao [286], Hakim [287], Miqueu [288]
Vapor Diffusion Coefficient	Lapuerta [289]	Slattery-Bird[290], Elliott-Watts [291]
Liquid Diffusion Coefficient	Wilke-Chang [292], Miyabe-Isogai [293]	
Hildebrand Solubility Parameter	Stefanis-Panayiotou [294]	
Octanol-Water Partition Coefficient	Klopman [295]	
Parachor	Sugden [296], Mumford-Phillips [297], Quayle [298], Gharagheizi [104]	Hugill-van Welsenes [299]

a: The Mani method was developed by Aspen Technologies™.

In the context of modeling pyrolysis bio-oils, Fonts et al. [217] and Manrique et al. [130] discussed methods and estimated properties for model components relevant to their work. In extension of their work, Fonseca [118] conducted a study of several of the property methods presented in Table 11 with a focus on deviations between experimental data and predicted results for 45 compounds typically found in pyrolysis condensates. The average relative deviation (estimated value vs experimental data) for each case is presented in Table 12 and Table 13, as well as the case for which each method produced the highest deviation to the experimental data. The full list of results and methods is available in the Supplementary Information. Comparing the estimated properties among each other, it is clear that there is a large discrepancy in performance of the methods when estimating a single parameter or variations with the temperature. For the latter, one has to be aware of the interval of validity of the regressions, which may not match the range for which experimental data is available, leading to high deviations. When analysing the worst cases, the influence of the shortcomings of group contribution methods becomes clear: some intramolecular phenomena are not correctly modeled by regressed parameters, which might be at play for small oxygenates. Other shortcomings of group contribution methods include the lack of groups to model certain structures, for example ketene (>C=C=O) groups. It is important to keep in mind that the Mani method and the TDE results are only obtainable making use of proprietary software and may not be available to all potential users, but were added here for the sake of comparison.

Table 12. Average relative deviations between predicted values and experimental data for some thermophysical properties for the group presented in Table 9 and Table 10. Adapted from data associated with [118]. Values in parenthesis refer to the number of components considered for the average. Part 1 of 2.

	Group contribution methods						Other methods/sources			
Normal Boiling Point (°C)	Joback	Gani	Cordes-Rarey				TDE [a]	ACD/Labs [b]	Stein-Brown [c]	Mani [d]
	3.9% (31)	4.5% (31)	6.3% (31)				1.4% (31)	1.5% (31)	3.8% (31)	3.1% (19)
Worst case	Linoleic Acid (52.2%)	Linoleic Acid (24.4%)	Glyoxal (34.1%)				Linoleic Acid (23.6%)	Linoleic Acid (26.1%)	Linoleic Acid (31.8%)	Furfural (76.0%)
Critical Temperature (°C)	Joback	Gani	Nannoolal-Rarey	Lydersen	Ambrose	Fedors	TDE [a]	Mani [d]		
	1.8% (17)	1.6% (17)	2.1% (17)	2.1% (17)	2.7% (17)	1.6% (17)	1.4% (17)	0.8% (8)		
Worst case	Linoleic Acid (19.5%)	Ethylene Glycol (17.6%)	Linoleic Acid (28.7%)	Linoleic Acid (18.6%)	Acetaldehyde (23.9%)	Ethylene Glycol (14.9%)	Furfuryl Alcohol (4.7%)	Furfural (23.1%)		
Critical Pressure (bar)	Joback	Gani	Nannoolal-Rarey	Lydersen	Ambrose		TDE [a]			
	4.6% (17)	5.8% (17)	4.2% (17)	6.9% (17)	22.1% (17)		7.8% (17)			
Worst case	Linoleic Acid (89.4%)	Linoleic Acid (89.6%)	Linoleic Acid (65.8%)	Linoleic Acid (88.6%)	Furfuryl Alcohol (464.1%)		Formic acid (108.2%)			
Critical Volume (cm^3/mol)	Joback	Gani	Nannoolal-Rarey	Lydersen	Ambrose	Fedors	TDE [a]			
	1.8% (14)	1.6% (14)	1.7% (14)	2.6% (14)	7.1% (14)	2.4% (14)	1.9% (14)			
Worst case	Formic acid (14.8%)	Phenol (15.3%)	Phenol (24.7%)	Formaldyehyde (28.7%)	Acetaldehyde (49.5%)	Phenol (23.0%)	p-Cresol (26.6%)			
Enthalpy of Vaporization (kJ/mol) @ T_b	Gani	Vetere	Ducros	Li-Ma	Clausius-Clayperon		TDE [a]	ACD/labs [b]		
	12.0% (21)	10.9% (21)	12.5% (21)	2.8% (9)	10.3% (9)		30.7% (18)	6.8% (20)		
Worst case	Acetic acid (95.8%)	Acetic acid (59.5%)	Ethylene Glycol (99.0%)	Glycol aldehyde (36.9%)	Acetic acid (74.7%)		Formaldehyde (202.6%)	Glycol aldehyde (38.6%)		

a: Estimated using the NIST ThermoDataEngine (TDE)® software. Available within Aspen Properties V14®.

b: Estimated using the Physchem Suite within the ACD/Labs™ Percepta® software. Available through ChemSpider (chemspider.com).

c: Adapted Stein-Brown method estimated using the US Environmental Protection Agency's EPISuite™. Available through ChemSpider (chemspider.com).

d: The Mani method was developed by Aspen Technologies™. Available within Aspen Properties V14®.

Table 13. Average relative deviations between predicted values and experimental data for some thermophysical properties for the group presented in Table 9 and Table 10. Adapted from data associated with [118]. Values in parenthesis refer to the number of components considered for the average. Part 2 of 2.

Ideal Gas Heat Capacity (J/mol.K) @ 25 °C	Joback	Benson	TDE [a]		Liquid Heat Capacity (J/mol.K) @ 25 °C	Růžička	TDE [a]
	6.5% (19)	6.2% (19)	3.0% (16)			7.6% (17)	0.4% (4)
Worst case	Acetone (85.3%)	Acetone (84.8%)	HMF (74.2%)		Worst case	Propanoic acid (112.5%)	Formaldehyde (17.4%)
Standard Enthalpy of Formation (kJ/mol)	Joback	Gani	Benson	TDE [a]	$\log K_{OW}$	Klopman	ACD/labs [b]
	28.7% (27)	24.4% (27)	24.3% (27)	0.0% (5)		15.5% (6)	6.8% (20)
Worst case	Linoleic Acid (732.2%)	Linoleic Acid (747.8%)	Linoleic Acid (729.8%)	Acetone (0.4%)	Worst case	Acetic acid (350.0%)	Glycol aldehyde (38.6%)
Standard liquid volume (cm3/mol)	Le-Bas	TDE [a]	Gunn-Yamada	ACD/Labs [b]	Heidelberg Solubility ($MPa^{1/2}$)	Stefanis-Panayiotou	TDE [a]
	20.8% (19)	3.7% (19)	19.7% (19)	3.8% (31)		2.6% (11)	2.2% (9)
Worst case	4-methylguaiacol (74.5%)	Acetaldehyde (22.3%)	4-methylguaiacol (70.5%)	Acetaldehyde (19.8%)	Worst case	Acetol (32.3%)	Acetol (45.7%)

a: Estimated using the NIST ThermoDataEngine (TDE)® software.
b: Estimated using the Physchem Suite within the ACD/Labs™ Percepta® software. Available through ChemSpider (chemspider.com).
c: Adapted Stein-Brown method estimated using the US Environmental Protection Agency's EPISuite™. Available through ChemSpider (chemspider.com).
d: Estimated using KOWWIN v1.67 within the US Environmental Protection Agency's EPISuite™. Available through ChemSpider (chemspider.com).

,

Specific to the vapor pressure (Table 14), it is sometimes difficult to discuss the feasibility of an estimation method for various different components. As in all other cases, high deviations arise from the temperature range of validity of the regressions and the available experimental data.

Table 14. Average relative deviations between predicted values and experimental data for the vapor pressure ofcompounds presented in **Table 9** and **Table 10**. Range of validity: 0-150 °C. Adapted from data associated with [118].

	Riedel	**Li-Ma**	**Mani**	**Nannoolal-Rarey**	**TDE**
Cummulative Deviation (CI 95%) [kPa]	65.1 ± 42.5	1065.9 ± 382.5	29.3 ± 13.6	47.2 ± 20.0	10.3 ± 7.0
Number of Points	31	26	26	31	29
Worse case	4-methylguaiacol	Glycol Aldehyde	Furfural	4-methylguaiacol	1-Propanaldehyde

Mixing rules are required to allow for the estimation of thermophysical properties of the phase mixture at the desired set of conditions. Most phase equilibria models consider the fluid as a single entity for which properties must be estimated using mixing rules. The enthalpy of a stream is a direct function of the process conditions (temperature, pressure, chemical potential) and can be estimated as a weighted sum of the enthalpy of each component present in each phase within the stream. The fraction of each component with the stream is typical a function of its fugacity. The enthalpy of each component is typically estimated using Hess's law, which considers factors such as the standard enthalpy of formation, sensible enthalpy at ideal gas phase, and enthalpy of phase change. However, it's also possible to estimate enthalpy based on values compiled for condensed phases.

Moreover, it is often relevant to know the properties of a given mixture stream (e.g., density, viscosity), for which properties are estimated by mixing rules. Most frequently, mixture properties are taken as weighed averages (Eq. 16), n=1), power laws (Eq. 16), n≠1) or logarithmic weighed averages (Eq. 17)) of the individual components. In Eq. 16) and Eq. 17), x_i^α refers to the molar fraction of component *i* in phase *α*, and X_i^α refers to the value of the property *X* for that same component *i* in phase *α* [54]. Gas-phase mixture properties are frequently estimated as a function of the properties of individual components and binary interaction parameters, based on simplifications of formal kinetic theory. [300] A summary of mixing rules is provided in **Table 15**.

.

$$X_m^{\alpha\,n} = \sum_i x_i^\alpha X_i^{\alpha\,n} \qquad 16)$$

$$\ln X_m^\alpha = \sum_{i=1}^{c} x_i^\alpha \, \ln X_i^\alpha \qquad 17)$$

Table 15. List of methods for estimation of mixture properties. Not extensive.

	Vapor-phase	**Liquid-phase**
Mixture Property	Estimation method	Estimation method
Thermal conductivity	Wassiljeva-Mason-Saxena [300]	Linear Weighted Average [301]
	Yoon-Thodos [302]	Vredeveld [301]
	Stiel-Thodos [303]	Wassiljeva [301]
	Hirschfelder-Eucken [300]	Chung-Lee-Starling [304]
	Schreiber-Vesovic-Wakeham [300]	Teja-Rice [305]

Viscosity	Ely-Hanley [306]	Logarithmic Weighted Average [54]
	Chapman-Enskog-Brokaw [307]	Modified Andrade [54]
	Chung-Lee-Starling [304]	McAllister [308]
	Wilke [309]	
	Davidson [310]	
	Lucas [54]	
Diffusion Coefficient	Chapman-Enskog-Wilke-Lee [289]	Wilke-Chang [292]
	Dawson-Khoury-Kobayashi [54]	
	Fuller [311]	
Molar Volume	Based on EoS	Modified Rackett-Spencer-Danner [54,268,312]
Surface Tension	-	Linear Weighted Average [54]
	-	Powerlaw Weighted Average [54]
	-	Modified MacLeod-Sugden [54]
		Zuo-Stenby [285]

Predicting thermophysical properties of components and mixtures, particularly pyrolysis condensates, can be challenging but are required since several thermophysical properties that are needed to run phase equilibria models are missing. Several approaches have been developed to address this challenge, among which group contribution methods take center-stage due to their ease of implementation. However, these methods rely on simplified assumptions and require careful selection of appropriate parameters. The most difficult parameters to estimate are also the most sensitive ones: those that vary with process conditions. There is no single approach that can accurately predict each thermophysical property of novel compounds or complex mixtures under all conditions; however, a combination of methods may be able to provide a comprehensive understanding of the behavior of these systems. In that case they represent a reasonable alternative if experimental data is missing.

Conclusion

In light of the escalating development in pyrolysis bio-oil applications, particularly with diverse feedstocks beyond pristine wood, there is an imperative need for the design of efficient refining processes. This necessitates the utilization of established separation technologies and, consequently, underscores the demand for reliable phase equilibrium models adept at handling the intricate composition of pyrolysis bio-oil. While existing phase equilibrium models represent the current pinnacle of sophistication, addressing the specific challenges intrinsic to pyrolysis bio-oil is crucial. This review has focused on four pivotal aspects related to liquid-vapor equilibrium (LVE), which is pertinent for both condensation design and distillation processes: the selection of an appropriate phase equilibrium model, formulation of a suitable surrogate mixture for pyrolysis bio-oil, characterization of the predominantly unknown high-molecular-weight (HMW) residue fraction, and estimation of absent thermophysical properties for compounds relevant to thermochemical liquefaction products.

Despite a discernible inclination towards activity coefficient models based on the context at hand, a broad spectrum of phase equilibrium models has been employed in the literature. While a definitive evaluation remains elusive due to a scarcity of experimental data, it becomes apparent that consideration of a non-ideal mixture in the liquid phase is imperative. Simultaneously, the reliability of activity coefficient models, such as UNIFAC-based models, is cast into doubt by the absence of experimental data necessary for refining binary interactions in relation to pyrolysis bio-oil compounds.

The selection of a surrogate mixture emerges as a critical decision contingent upon the goals of the modeling study. The necessity for such a surrogate mixture arises from both the presence of a substantial fraction of unknown components and the dearth of reliable, compound-specific data, which adversely impacts the precision of resultant models. It is evident that diverse surrogate mixtures will coexist in the future. Analogous to the choice of phase equilibrium models, a comprehensive analysis of the suitability of various approaches is impeded by a lack of experimental data. A judicious selection of a pyrolysis bio-oil surrogate mixture should account for the HMW residue, whose chemical composition remains largely elusive. This consideration is pivotal not only for representing its significant weight fraction but also for acknowledging its interaction with other more volatile molecules, such as water, influencing their behavior in phase equilibria.

The paucity of thermophysical properties for compounds relevant to pyrolysis bio-oil poses a substantial challenge. This necessitates the estimation of these properties, resulting in values of lesser reliability compared to experimental data. No clear consensus emerges regarding the most reliable estimation method, suggesting that a combination of diverse approaches could enhance the precision of the overall model.

To propel this field forward, it is imperative to augment the availability of reliable experimental phase equilibrium data for pyrolysis bio-oil and its constituent compounds, alongside their thermophysical properties. This collective effort will undoubtedly contribute to refining and advancing the modeling approaches essential for the efficient utilization of pyrolysis bio-oil in diverse applications.

AUTHOR INFORMATION

Corresponding Author

Dr. Axel Funke (axel.funke@kit.edu)

Author Contributions

The manuscript was written through contributions of all authors. All authors have given approval to the final version of the manuscript.

ABBREVIATIONS

Acronyms: BO, Bio-oil; CF, Computational fluid dynamics; DEM, Discrete element method(s); DMD, Dortmund variant of the UNIFAC method; EoS;Equation of State; GCA, Group Contribution with Association EoS method; HOC, Hayden O'Connell EoS method; LVE, Liquid-vapor equilibrium; NRTL, Non-Random Two Liquids method; PR, Peng-Robinson EoS method; PR-BM, Peng-Robinson EoS method with Boston-Matthias mixing rules; RK, Redlich-Kwong EoS method; SAFT, Statistical Associating Fluid Theory EoS method; SRK-BM, Soave-Redlich-Kwong EoS method with Boston-Matthias mixing rules; SRK-KD, Soave-Redlich-Kwong EoS method with Kabadi-Danner mixing rules; UNIFAC, UNIQUAC Functional-group Activity Coefficients method; UNIQUAC, Universal Quasichemical method.

Latin letters: F, Fugacity; G, Gibbs energy; P, Pressure; T, Temperature; U, Internal energy; n, Number of moles; x, Molar fraction.

Greek letters: Φ, Fugacity coefficient; μ, Chemical potential; ν Stoichiometric number

Offscript symbols: i, Individual chemical species; V, Vapor-phase property; L, Liquid-phase property.

ABBREVIATIONS

(1) BP p.l.c. *BP Statistical Review of World Energy 2018*; London, UK, 2018.

(2) IRENA; IEA Bioenergy; FAO. *Bioenergy for Sustainable Development*; 2017.

(3) Basu, P. *Biomass Gasification and Pyrolysis: Practical Design and Theory*; Elsevier, 2010.

(4) Lappalainen, J.; Baudouin, D.; Hornung, U.; Schuler, J.; Melin, K.; Bjelić, S.; Vogel, F.; Konttinen, J.; Joronen, T. Sub- and Supercritical Water Liquefaction of Kraft Lignin and Black Liquor Derived Lignin. *Energies (Basel)* **2020**, *13* (13), 3309. https://doi.org/10.3390/en13133309.

(5) Pimenta, A. S.; Gama, G. S. P.; Feijó, F. M. C.; Braga, R. M.; de Azevedo, T. K. B.; de Melo, R. R.; de Oliveira Miranda, N.; de Andrade, G. S. Wood Vinegar from Slow

Pyrolysis of Eucalyptus Wood: Assessment of Removing Contaminants by Sequential Vacuum Distillation. *Forests* **2023**, *14* (12), 2414. https://doi.org/10.3390/f14122414.

(6) Westerhof, R. J. M.; Brilman, D. W. F.; Garcia-Perez, M.; Wang, Z.; Oudenhoven, S. R. G.; Van Swaaij, W. P. M.; Kersten, S. R. A. Fractional Condensation of Biomass Pyrolysis Vapors. *Energy and Fuels* **2011**, *25* (4), 1817–1829. https://doi.org/10.1021/ef2000322.

(7) Schmitt, C. C. C. C.; Moreira, R.; Neves, R. C. R. C.; Richter, D.; Funke, A.; Raffelt, K.; Grunwaldt, J.-D. J.-D. D.; Dahmen, N. From Agriculture Residue to Upgraded Product: The Thermochemical Conversion of Sugarcane Bagasse for Fuel and Chemical Products. *Fuel Processing Technology* **2020**, *197* (June 2019), 106199. https://doi.org/10.1016/j.fuproc.2019.106199.

(8) Alburquerque, J. A.; Sánchez, M. E.; Mora, M.; Barrón, V. Slow Pyrolysis of Relevant Biomasses in the Mediterranean Basin. Part 2. Char Characterisation for Carbon Sequestration and Agricultural Uses. *J Clean Prod* **2016**, *120*, 191–197. https://doi.org/10.1016/j.jclepro.2014.10.080.

(9) Funke, A.; Niebel, A.; Richter, D.; Abbas, M. M.; Müller, A. K.; Radloff, S.; Paneru, M.; Maier, J.; Dahmen, N.; Sauer, J. Fast Pyrolysis Char - Assessment of Alternative Uses within the Bioliq® Concept. *Bioresour Technol* **2016**, *200*, 905–913. https://doi.org/10.1016/j.biortech.2015.11.012.

(10) Van de Velden, M.; Baeyens, J.; Brems, A.; Janssens, B.; Dewil, R. Fundamentals, Kinetics and Endothermicity of the Biomass Pyrolysis Reaction. *Renew Energy* **2010**, *35* (1), 232–242. https://doi.org/10.1016/j.renene.2009.04.019.

(11) Satya, K. K. P. V. Computational Modelling of the Condensation Process of the Fast Pyrolysis Vapours in Liquid Collection Systems. Doctor of Philosophy, University of Liverpool, Liverpool, 2015.

(12) Meier, D.; Van De Beld, B.; Bridgwater, A. V.; Elliott, D. C.; Oasmaa, A.; Preto, F. State-of-the-Art of Fast Pyrolysis in IEA Bioenergy Member Countries. *Renewable and Sustainable Energy Reviews* **2013**, *20*, 619–641. https://doi.org/10.1016/j.rser.2012.11.061.

(13) Papari, S.; Hawboldt, K. A Review on Condensing System for Biomass Pyrolysis Process. *Fuel Processing Technology*. Elsevier B.V. November 1, 2018, pp 1–13. https://doi.org/10.1016/j.fuproc.2018.08.001.

(14) Pfitzer, C.; Dahmen, N.; Tröger, N.; Weirich, F.; Sauer, J.; Günther, A.; Müller-Hagedorn, M. Fast Pyrolysis of Wheat Straw in the Bioliq Pilot Plant. *Energy and Fuels* **2016**, *30* (10), 8047–8054. https://doi.org/10.1021/acs.energyfuels.6b01412.

(15) Funke, A.; Tomasi Morgano, M.; Leibold, H.; Dahmen, N.; Leibold, H. Experimental Comparison of Two Bench Scale Units for Fast and Intermediate Pyrolysis. *J Anal Appl Pyrolysis* **2017**, *124*, 504–514. https://doi.org/10.1016/j.jaap.2016.12.033.

(16) Tröger, N.; Richter, D.; Stahl, R. Effect of Feedstock Composition on Product Yields and Energy Recovery Rates of Fast Pyrolysis Products from Different Straw Types. *J Anal Appl Pyrolysis* **2013**, *100*, 158–165. https://doi.org/10.1016/j.jaap.2012.12.012.

(17) Brigagão, G. V.; de Queiroz Fernandes Araújo, O.; de Medeiros, J. L.; Mikulcic, H.; Duic, N. A Techno-Economic Analysis of Thermochemical Pathways for Corncob-to-

Energy: Fast Pyrolysis to Bio-Oil, Gasification to Methanol and Combustion to Electricity. *Fuel Processing Technology* **2019**, *193*, 102–113. https://doi.org/10.1016/j.fuproc.2019.05.011.

(18) Kim, P.; Weaver, S.; Labbé, N. Effect of Sweeping Gas Flow Rates on Temperature-Controlled Multistage Condensation of Pyrolysis Vapors in an Auger Intermediate Pyrolysis System. *J Anal Appl Pyrolysis* **2016**, *118*, 325–334. https://doi.org/10.1016/j.jaap.2016.02.017.

(19) Fonseca, F. G.; Funke, A.; Niebel, A.; Soares Dias, A. P.; Dahmen, N. Moisture Content as a Design and Operational Parameter for Fast Pyrolysis. *J Anal Appl Pyrolysis* **2019**, *139*, 73–86. https://doi.org/10.1016/j.jaap.2019.01.012.

(20) Williams, P. T.; Brindle, A. J. Temperature Selective Condensation of Tyre Pyrolysis Oils to Maximise the Recovery of Single Ring Aromatic Compounds. *Fuel* **2003**, *82* (9), 1023–1031. https://doi.org/10.1016/S0016-2361(03)00016-4.

(21) Parku, G. K.; Krutof, A.; Funke, A.; Richter, D.; Dahmen, N. Using Fractional Condensation to Optimize Aqueous Pyrolysis Condensates for Downstream Microbial Conversion. *Ind Eng Chem Res* **2023**, *62* (6), 2792–2803. https://doi.org/10.1021/acs.iecr.2c03598.

(22) Kubisch, C.; Ochsenreither, K. Detoxification of a Pyrolytic Aqueous Condensate from Wheat Straw for Utilization as Substrate in Aspergillus Oryzae DSM 1863 Cultivations. *Biotechnology for Biofuels and Bioproducts* **2022**, *15* (1), 18. https://doi.org/10.1186/s13068-022-02115-z.

(23) Kövilein, A.; Kubisch, C.; Cai, L.; Ochsenreither, K. Malic Acid Production from Renewables: A Review. *Journal of Chemical Technology & Biotechnology* **2020**, *95* (3), 513–526. https://doi.org/10.1002/jctb.6269.

(24) Dias, I. A.; Horta, R. P.; Matos, M.; Helm, C. V.; Magalhães, W. L. E.; Lima, E. A.; Silva, B. J. G.; Muniz, G. I. B.; Cademartori, P. H. G. Bioproducts from the Pyrolytic Lignin Separation of Fast-Pyrolysis Bio-Oil: Potential of Water-Soluble Fraction Generated in a Simple Cold-Water Extraction Method.

(25) Ranzi, E.; Debiagi, P. E. A.; Frassoldati, A. Mathematical Modeling of Fast Biomass Pyrolysis and Bio-Oil Formation. Note I: Kinetic Mechanism of Biomass Pyrolysis. *ACS Sustain Chem Eng* **2017**, *5* (4), 2867–2881. https://doi.org/10.1021/ACSSUSCHEMENG.6B03096/ASSET/IMAGES/SC-2016-03096M_M014.GIF.

(26) Qi, Y.; Fu, P.; Volmer, D. A. Analysis of Natural Organic Matter via Fourier Transform Ion Cyclotron Resonance Mass Spectrometry: An Overview of Recent Non-Petroleum Applications. *Mass Spectrom Rev* **2022**, *41* (5), 647–661. https://doi.org/10.1002/MAS.21634.

(27) Scholze, B.; Meier, D. Characterization of the Water-Insoluble Fraction from Pyrolysis Oil (Pyrolytic Lignin). Part I. PY-GC/MS, FTIR, and Functional Groups. *J Anal Appl Pyrolysis* **2001**, *60* (1), 41–54. https://doi.org/10.1016/S0165-2370(00)00110-8.

(28) Scholze, B.; Hanser, C.; Meier, D. Characterization of the Water-Insoluble Fraction from Fast Pyrolysis Liquids (Pyrolytic Lignin). Part II: GPC, Carbonyl Groups, and 13C-

NMR. *J Anal Appl Pyrolysis* **2001**, *58–59*, 387–400. https://doi.org/10.1016/S0165-2370(00)00173-X.

(29) Bayerbach, R.; Nguyen, V. D.; Schurr, U.; Meier, D. Characterization of the Water-Insoluble Fraction from Fast Pyrolysis Liquids (Pyrolytic Lignin). Part III: Molar Mass Characteristics by SEC, MALDI-TOF-MS, LDI-TOF-MS, and Py-FIMS. *J Anal Appl Pyrolysis* **2006**, *77* (2), 95–101. https://doi.org/10.1016/j.jaap.2006.02.002.

(30) Bayerbach, R.; Meier, D. Characterization of the Water-Insoluble Fraction from Fast Pyrolysis Liquids (Pyrolytic Lignin). Part IV: Structure Elucidation of Oligomeric Molecules. *J Anal Appl Pyrolysis* **2009**, *85* (1–2), 98–107. https://doi.org/10.1016/j.jaap.2008.10.021.

(31) Schmitt, C. C.; Fonseca, F. G.; Fraga, M. M. C.; Wisniewski, A.; Karp, S.; Mello José, Á. H.; Rodrigues, R. C. L. B.; Moreira, R.; Hirayama, D. E.; Raffelt, K.; Dahmen, N.; Jr, A. W.; Karp, S.; Henrique, Á.; José, M.; Rita, C.; Moreira, R.; Eiji, D.; Raffelt, K.; Dahmen, N. Thermochemical and Catalytic Conversion Technologies for the Development of Brazilian Biomass Utilization. *Catalysts* **2021**, *11* (12), 1549. https://doi.org/10.3390/catal11121549.

(32) Fonseca, F. G.; Funke, A.; Niebel, A.; Dias, A. P. S.; Dahmen, N. Moisture Content as a Design and Operational Parameter for Fast Pyrolysis. In *1. Deutsches Doktorandenkolloquium Bioenergie*; DBFZ Deutsches Biomasseforschungszentrum gemeinnützige GmbH, 2018; p 286.

(33) Şen, A. U.; Fonseca, F. G.; Funke, A.; Pereira, H.; Lemos, F. Pyrolysis Kinetics and Estimation of Chemical Composition of Quercus Cerris Cork. *Biomass Convers Biorefin* **2020**. https://doi.org/10.1007/s13399-020-00964-y.

(34) Gustavsson, C.; Nilsson, L. Co-Production of Pyrolysis Oil in District Heating Plants: Systems Analysis of Dual Fluidized-Bed Pyrolysis with Sequential Vapor Condensation. *Energy and Fuels* **2013**, *27* (9), 5313–5319. https://doi.org/10.1021/ef401143v.

(35) Scholze, B.; Meier, D. Characterization of the Water-Insoluble Fraction from Pyrolysis Oil (Pyrolytic Lignin). Part I. PY–GC/MS, FTIR, and Functional Groups. *J Anal Appl Pyrolysis* **2001**, *60* (1), 41–54. https://doi.org/10.1016/S0165-2370(00)00110-8.

(36) Figueirêdo, M. B.; Hita, I.; Deuss, P. J.; Venderbosch, R. H.; Heeres, H. J. Pyrolytic Lignin: A Promising Biorefinery Feedstock for the Production of Fuels and Valuable Chemicals. *Green Chemistry* **2022**, *24* (12), 4680–4702. https://doi.org/10.1039/D2GC00302C.

(37) Ille, Y.; Kröhl, F.; Velez, A.; Funke, A.; Pereda, S.; Schaber, K.; Dahmen, N. Activity of Water in Pyrolysis Oil—Experiments and Modelling. *J Anal Appl Pyrolysis* **2018**, *135* (August), 260–270. https://doi.org/10.1016/j.jaap.2018.08.027.

(38) Wang, H.; Gunawan, R.; Wang, Z.; Zhang, L.; Liu, Y.; Wang, S.; Hasan, M. D. M.; Li, C.-Z. High-Pressure Reactive Distillation of Bio-Oil for Reduced Polymerisation. *Fuel Processing Technology* **2021**, *211*, 106590. https://doi.org/10.1016/j.fuproc.2020.106590.

(39) Nam, H.; Choi, J.; Capareda, S. C. Comparative Study of Vacuum and Fractional Distillation Using Pyrolytic Microalgae (Nannochloropsis Oculata) Bio-Oil. *Algal Res* **2016**, *17*, 87–96. https://doi.org/10.1016/j.algal.2016.04.020.

(40) Rahman, S.; Helleur, R.; MacQuarrie, S.; Papari, S.; Hawboldt, K. Upgrading and Isolation of Low Molecular Weight Compounds from Bark and Softwood Bio-Oils through Vacuum Distillation. *Sep Purif Technol* **2018**, *194*, 123–129. https://doi.org/10.1016/j.seppur.2017.11.033.

(41) Cláudio, A. F. M.; Freire, M. G.; Freire, C. S. R.; Silvestre, A. J. D.; Coutinho, J. A. P. Extraction of Vanillin Using Ionic-Liquid-Based Aqueous Two-Phase Systems. *Sep Purif Technol* **2010**, *75* (1), 39–47. https://doi.org/10.1016/j.seppur.2010.07.007.

(42) Li, X.; Kersten, S. R. A.; Schuur, B. Extraction of Guaiacol from Model Pyrolytic Sugar Stream with Ionic Liquids. *Ind Eng Chem Res* **2016**, *55* (16), 4703–4710. https://doi.org/10.1021/acs.iecr.6b00100.

(43) Bharti, A.; Kundu, D.; Rabari, D.; Banerjee, T. Liquid–Liquid Equilibria: Experiments, Correlation and Prediction. In *Phase Equilibria in Ionic Liquid Facilitated Liquid–Liquid Extractions*; CRC Press: Boca Raton, FL : CRC Press, Taylor & Francis Group, [2017], 2017; pp 9–52. https://doi.org/10.1201/9781315367163-2.

(44) Pavón, S.; Blaesing, L.; Jahn, A.; Aubel, I.; Bertau, M. Liquid Membranes for Efficient Recovery of Phenolic Compounds Such as Vanillin and Catechol. *Membranes (Basel)* **2020**, *11* (1), 20. https://doi.org/10.3390/membranes11010020.

(45) Cichy, W.; Schlosser, S.; Szymanowski, J. Recovery of Phenol with Cyanex® 923 in Membrane Extraction-Stripping Systems. *Solvent Extraction and Ion Exchange* **2001**, *19* (5), 905–923. https://doi.org/10.1081/SEI-100107029.

(46) Zidi, C.; Tayeb, R.; Dhahbi, M. Extraction of Phenol from Aqueous Solutions by Means of Supported Liquid Membrane (MLS) Containing Tri-n-Octyl Phosphine Oxide (TOPO). *J Hazard Mater* **2011**, *194*, 62–68. https://doi.org/10.1016/j.jhazmat.2011.07.071.

(47) Rosly, M. B.; Jusoh, N.; Othman, N.; Rahman, H. A.; Sulaiman, R. N. R.; Noah, N. F. M. Stability of Emulsion Liquid Membrane Using Bifunctional Diluent and Blended Nonionic Surfactant for Phenol Removal. *Chemical Engineering and Processing - Process Intensification* **2020**, *148*, 107790. https://doi.org/10.1016/j.cep.2019.107790.

(48) Guo, X.; Wang, S.; Guo, Z.; Liu, Q.; Luo, Z.; Cen, K. Pyrolysis Characteristics of Bio-Oil Fractions Separated by Molecular Distillation. *Appl Energy* **2010**, *87* (9), 2892–2898. https://doi.org/10.1016/j.apenergy.2009.10.004.

(49) Zhang, M.; Wu, H. Pyrolytic Lignin from Fast Pyrolysis Bio-Oil via Cold-Water Precipitation: Optimal Separation Conditions and Properties. *Fuel* **2019**, *242*, 580–586. https://doi.org/10.1016/j.fuel.2019.01.092.

(50) Oasmaa, A.; Lehto, J.; Solantausta, Y.; Kallio, S. Historical Review on VTT Fast Pyrolysis Bio-Oil Production and Upgrading. *Energy & Fuels* **2021**, *35* (7), 5683–5695. https://doi.org/10.1021/acs.energyfuels.1c00177.

(51) Gani, R.; O'Connell, J. P. Chapter 2: Role of Properties and Their Models in Process and Product Design. In *Computer Aided Chemical Engineering*; Elsevier, 2004; Vol. 19, pp 27–41. https://doi.org/10.1016/S1570-7946(04)80004-X.

(52) Carlson, E. Don't Gamble With Physical Properties For Simulations. *Chem Eng Prog* **1996**, No. October, 35–46.

(53) Pereda, S.; Brignole, E.; Bottini, S. Chapter 13. Equations of State in Chemical Reacting Systems. In *Applied Thermodynamics of Fluids*; Royal Society of Chemistry: Cambridge, 2010; pp 433–459. https://doi.org/10.1039/9781849730983-00433.

(54) Aspen Technology Inc. Aspen Physical Property System: Physical Property Methods. Bedford, USA 2016.

(55) Cengel, Y. A.; Boles, M. A. *Thermodyamics: An Engineering Approach*, 6th ed.; McGraw-Hill, 2007; Vol. 1.

(56) Redlich, Otto.; Kwong, J. N. S. On the Thermodynamics of Solutions. V. An Equation of State. Fugacities of Gaseous Solutions. *Chem Rev* **1949**, *44* (1), 233–244. https://doi.org/10.1021/cr60137a013.

(57) Péneloux, A.; Rauzy, E.; Fréze, R. A Consistent Correction for Redlich-Kwong-Soave Volumes. *Fluid Phase Equilib* **1982**, *8* (1), 7–23. https://doi.org/10.1016/0378-3812(82)80002-2.

(58) Knudsen, K. Phase Equilibria and Transport of Multiphase Systems, Technical University of Denmark, 1992.

(59) Neau, E.; Hernández-Garduza, O.; Escandell, J.; Nicolas, C.; Raspo, I. The Soave, Twu and Boston–Mathias Alpha Functions in Cubic Equations of State. *Fluid Phase Equilib* **2009**, *276* (2), 87–93. https://doi.org/10.1016/j.fluid.2008.09.023.

(60) Lopez-Echeverry, J. S.; Reif-Acherman, S.; Araujo-Lopez, E. Peng-Robinson Equation of State: 40 Years through Cubics. *Fluid Phase Equilib* **2017**, *447*, 39–71. https://doi.org/10.1016/j.fluid.2017.05.007.

(61) Kontogeorgis, G. M.; Voutsas, E. C.; Yakoumis, I. V.; Tassios, D. P. An Equation of State for Associating Fluids. *Ind Eng Chem Res* **1996**, *35* (11), 4310–4318. https://doi.org/10.1021/ie9600203.

(62) Kontogeorgis, G. M.; Liang, X.; Arya, A.; Tsivintzelis, I. Equations of State in Three Centuries. Are We Closer to Arriving to a Single Model for All Applications? *Chemical Engineering Science: X* **2020**, *7*, 100060. https://doi.org/10.1016/j.cesx.2020.100060.

(63) Eslami, L.; Khadem-Hamedani, B. Development of a Novel Peng–Robinson plus Association Equation of State for Industrially Important Associating Compounds. *Neural Comput Appl* **2019**, *31* (7), 2107–2115. https://doi.org/10.1007/s00521-015-2126-2.

(64) Mathias, P. M.; Copeman, T. W. Extension of the Peng-Robinson Equation of State to Complex Mixtures: Evaluation of the Various Forms of the Local Composition Concept. *Fluid Phase Equilib* **1983**, *13*, 91–108. https://doi.org/10.1016/0378-3812(83)80084-3.

(65) Schwartzentruber, J.; Renon, H.; Watanasiri, S. Development of a New Cubic Equation of State for Phase Equilibrium Calculations. *Fluid Phase Equilib* **1989**, *52*, 127–134. https://doi.org/10.1016/0378-3812(89)80319-X.

(66) Holderbaum, T.; Gmehling, J. PSRK: A Group Contribution Equation of State Based on UNIFAC. *Fluid Phase Equilib* **1991**, *70* (2–3), 251–265. https://doi.org/10.1016/0378-3812(91)85038-V.

(67) Mathias, P. M. A Versatile Phase Equilibrium Equation of State. *Industrial & Engineering Chemistry Process Design and Development* **1983**, *22* (3), 385–391. https://doi.org/10.1021/i200022a008.

(68) Fischer, K.; Gmehling, J. Further Development, Status and Results of the PSRK Method for the Prediction of Vapor-Liquid Equilibria and Gas Solubilities. *Fluid Phase Equilib* **1995**, *112* (1), 1–22. https://doi.org/10.1016/0378-3812(95)02792-D.

(69) Huron, M.-J.; Vidal, J. New Mixing Rules in Simple Equations of State for Representing Vapour-Liquid Equilibria of Strongly Non-Ideal Mixtures. *Fluid Phase Equilib* **1979**, *3* (4), 255–271. https://doi.org/10.1016/0378-3812(79)80001-1.

(70) Michelsen, M. L. A Modified Huron-Vidal Mixing Rule for Cubic Equations of State. *Fluid Phase Equilib* **1990**, *60* (1–2), 213–219. https://doi.org/10.1016/0378-3812(90)85053-D.

(71) Vidal, J.; Bogdanić, G. Equations of State, Mixing Rules and Phase Equilibrium Calculations. Part 2. Mixing Rules and Vapor-Liquid Equilibrium Calculation. *Chem Biochem Eng Q* **1999**, *13* (3), 101–125.

(72) Kabadi, V. N.; Danner, R. P. A Modified Soave-Redlich-Kwong Equation of State for Water-Hydrocarbon Phase Equilibria. *Industrial & Engineering Chemistry Process Design and Development* **1985**, *24* (3), 537–541. https://doi.org/10.1021/i200030a004.

(73) Benedict, M.; Webb, G. B.; Rubin, L. C. An Empirical Equation for Thermodynamic Properties of Light Hydrocarbons and Their Mixtures I. Methane, Ethane, Propane and *n* -Butane. *J Chem Phys* **1940**, *8* (4), 334–345. https://doi.org/10.1063/1.1750658.

(74) Brulé, M. R.; Lin, C. T.; Lee, L. L.; Starling, K. E. Multiparameter Corresponding-States Correlation of Coal-Fluid Thermodynamic Properties. *AIChE Journal* **1982**, *28* (4), 616–625. https://doi.org/10.1002/aic.690280414.

(75) Lee, B. I.; Kesler, M. G. A Generalized Thermodynamic Correlation Based on Three-Parameter Corresponding States. *AIChE Journal* **1975**, *21* (3), 510–527. https://doi.org/10.1002/aic.690210313.

(76) Plöcker, U.; Knapp, H.; Prausnitz, J. Calculation of High-Pressure Vapor-Liquid Equilibria from a Corresponding-States Correlation with Emphasis on Asymmetric Mixtures. *Industrial & Engineering Chemistry Process Design and Development* **1978**, *17* (3), 324–332. https://doi.org/10.1021/i260067a020.

(77) Perry, R. H.; Maloney, J. O.; Green, D. W. *Perry's Chemical Engineers' Handbook*, 8th ed.; McGraw-Hill, 2008; Vol. 1. https://doi.org/10.1036/0071422943.

(78) Prausnitz, J. M.; Lichtenthaler, R. N.; Azevedo, E. G. de. Fugacities in Liquid Mixtures: Excess Functions. In *Molecular thermodynamics of fluid-phase equilibria*; Prentice-Hall: Englewood Cliffs, N.J., USA, 1986.

(79) Nothnagel, K. H.; Abrams, D. S.; Prausnitz, J. M. Generalized Correlation for Fugacity Coefficients in Mixtures at Moderate Pressures. Application of Chemical Theory of Vapor Imperfections. *Industrial and Engineering Chemistry Process Design and Development* **1973**, *12* (1), 25–35. https://doi.org/10.1021/i260045a006.

(80) Hayden, J. G.; O'Connell, J. P. A Generalized Method for Predicting Second Virial Coefficients. *Industrial & Engineering Chemistry Process Design and Development* **1975**, *14* (3), 209–216. https://doi.org/10.1021/i260055a003.

(81) Wertheim, M. S. Fluids with Highly Directional Attractive Forces. I. Statistical Thermodynamics. *J Stat Phys* **1984**, *35* (1–2), 19–34. https://doi.org/10.1007/BF01017362.

(82) Wertheim, M. S. Fluids with Highly Directional Attractive Forces. II. Thermodynamic Perturbation Theory and Integral Equations. *J Stat Phys* **1984**, *35* (1–2), 35–47. https://doi.org/10.1007/BF01017363.

(83) Wertheim, M. S. Fluids with Highly Directional Attractive Forces. III. Multiple Attraction Sites. *J Stat Phys* **1986**, *42* (3–4), 459–476. https://doi.org/10.1007/BF01127721.

(84) Wertheim, M. S. Fluids with Highly Directional Attractive Forces. IV. Equilibrium Polymerization. *J Stat Phys* **1986**, *42* (3–4), 477–492. https://doi.org/10.1007/BF01127722.

(85) Chapman, W. G.; Gubbins, K. E.; Jackson, G.; Radosz, M. SAFT: Equation-of-State Solution Model for Associating Fluids. *Fluid Phase Equilib* **1989**, *52*, 31–38. https://doi.org/10.1016/0378-3812(89)80308-5.

(86) Gross, J.; Sadowski, G. Application of Perturbation Theory to a Hard-Chain Reference Fluid: An Equation of State for Square-Well Chains. *Fluid Phase Equilib* **2000**, *168* (2), 183–199. https://doi.org/10.1016/S0378-3812(00)00302-2.

(87) Gross, J.; Sadowski, G. Perturbed-Chain SAFT: An Equation of State Based on a Perturbation Theory for Chain Molecules. *Ind Eng Chem Res* **2001**, *40* (4), 1244–1260. https://doi.org/10.1021/ie0003887.

(88) Gross, J.; Spuhl, O.; Tumakaka, F.; Sadowski, G. Modeling Copolymer Systems Using the Perturbed-Chain SAFT Equation of State. *Ind Eng Chem Res* **2003**, *42* (6), 1266–1274. https://doi.org/10.1021/ie020509y.

(89) Skjold-Joergensen, S. Group Contribution Equation of State (GC-EOS): A Predictive Method for Phase Equilibrium Computations over Wide Ranges of Temperature and Pressures up to 30 MPa. *Ind Eng Chem Res* **1988**, *27* (1), 110–118. https://doi.org/10.1021/ie00073a021.

(90) Novák, J. P.; Matouš, J.; Pick, J. *Liquid-Liquid Equilibria*; Elsevier, 1987.

(91) Margules, M. Über Die Zusammensetzung Der Gesättigten Dämpfe von Misschungen. In *Sitzungsberichte der Kaiserliche Akadamie der Wissenschaften Wien Mathematisch-Naturwissenschaftliche Klasse II*; Kaiserlich-Königlichen Hof- und Staatsdruckerei: Wien, 1895; Vol. 104, pp 1243–1278.

(92) Peng, D.-Y. Extending the Van Laar Model to Multicomponent Systems. *The Open Thermodynamics Journal* **2010**, *4* (1), 129–140. https://doi.org/10.2174/1874396X01004010129.

(93) Hiranuma, M. A New Expression Similar to the Three-Parameter Wilson Equation. *Industrial & Engineering Chemistry Fundamentals* **1974**, *13* (3), 219–222. https://doi.org/10.1021/i160051a010.

(94) Wilson, G. M. Vapor-Liquid Equilibrium. XI. A New Expression for the Excess Free Energy of Mixing. *J Am Chem Soc* **1964**, *86* (2), 127–130. https://doi.org/10.1021/ja01056a002.

(95) Renon, H.; Prausnitz, J. M. Local Compositions in Thermodynamic Excess Functions for Liquid Mixtures. *AIChE Journal* **1968**, *14* (1), 135–144. https://doi.org/10.1002/aic.690140124.

(96) Maurer, G.; Prausnitz, J. M. On the Derivation and Extension of the Uniquac Equation. *Fluid Phase Equilib* **1978**, *2* (2), 91–99. https://doi.org/10.1016/0378-3812(78)85002-X.

(97) Abrams, D. S.; Prausnitz, J. M. Statistical Thermodynamics of Liquid Mixtures: A New Expression for the Excess Gibbs Energy of Partly or Completely Miscible Systems. *AIChE Journal* **1975**, *21* (1), 116–128. https://doi.org/10.1002/aic.690210115.

(98) Anderson, T. F.; Prausnitz, J. M. Application of the UNIQUAC Equation to Calculation of Multicomponent Phase Equilibria. 1. Vapor-Liquid Equilibria. *Industrial & Engineering Chemistry Process Design and Development* **1978**, *17* (4), 552–561. https://doi.org/10.1021/i260068a028.

(99) Oasmaa, A.; Elliott, D. C.; Korhonen, J. Acidity of Biomass Fast Pyrolysis Bio-Oils. *Energy and Fuels* **2010**, *24* (12), 6548–6554. https://doi.org/10.1021/ef100935r.

(100) Fredenslund, A.; Jones, R. L.; Prausnitz, J. M. Group-contribution Estimation of Activity Coefficients in Nonideal Liquid Mixtures. *AIChE Journal* **1975**, *21* (6), 1086–1099. https://doi.org/10.1002/aic.690210607.

(101) Fredenslund, A.; Gmehling, J.; Rasmussen, P. *Vapor-Liquid Equilibria Using UNIFAC a Group-contribution Method*; Gaube, J., Ed.; Wiley-VCH Verlag GmbH & Co: Weinheim, Germany, 1977.

(102) Muzenda, E. From UNIQUAC to Modified UNIFAC Dortmund : A Discussion. In *3rd International Conference on Medical Sciences and Chemical Engineering (ICMSCE'2013)*; Bangkok, Thailand, 2013; pp 32–41.

(103) Magnussen, T.; Rasmussen, P.; Fredenslund, A. UNIFAC Parameter Table for Prediction of Liquid-Liquid Equilibria. *Industrial and Engineering Chemistry Process Design and Development* **1981**, *20* (2), 331–339. https://doi.org/10.1021/i200013a024.

(104) Gharagheizi, F.; Eslamimanesh, A.; Mohammadi, A. H.; Richon, D. Determination of Parachor of Various Compounds Using an Artificial Neural Network−Group Contribution Method. *Ind Eng Chem Res* **2011**, *50* (9), 5815–5823. https://doi.org/10.1021/ie102464t.

(105) Kikić, I.; Alessi, P.; Rasmussen, P.; Fredenslund, A. On the Combinatorial Part of the UNIFAC and UNIQUAC Models. *Can J Chem Eng* **1980**, *58* (2), 253–258. https://doi.org/10.1002/cjce.5450580218.

(106) Larsen, B. L.; Rasmussen, P.; Fredenslund, A. A Modified UNIFAC Group-Contribution Model for Prediction of Phase Equilibria and Heats of Mixing. *Ind Eng Chem Res* **1987**, *26* (11), 2274–2286. https://doi.org/10.1021/ie00071a018.

(107) Weidlich, U.; Gmehling, J. A Modified UNIFAC Model. 1. Prediction of VLE, HE, and Γ∞. *Ind Eng Chem Res* **1987**, *26* (7), 1372–1381. https://doi.org/10.1021/ie00067a018.

(108) Chen, Y.; Liu, X.; Woodley, J. M.; Kontogeorgis, G. M. Gas Solubility in Ionic Liquids: UNIFAC-IL Model Extension. *Ind Eng Chem Res* **2020**, *59* (38), 16805–16821. https://doi.org/10.1021/acs.iecr.0c02769.

(109) Dahl, S.; Michelsen, M. L. High-Pressure Vapor-Liquid Equilibrium with a UNIFAC-Based Equation of State. *AIChE Journal* **1990**, *36* (12), 1829–1836. https://doi.org/10.1002/aic.690361207.

(110) Van Ness, H. C.; Byer, S. M.; Gibbs, R. E. Vapor-Liquid Equilibrium: Part I. An Appraisal of Data Reduction Methods. *AIChE Journal* **1973**, *19* (2), 238–244. https://doi.org/10.1002/aic.690190206.

(111) Marcilla, A.; Reyes-Labarta, J. A.; Olaya, M. M. Should We Trust All the Published LLE Correlation Parameters in Phase Equilibria? Necessity of Their Assessment Prior to Publication. *Fluid Phase Equilib* **2017**, *433*, 243–252. https://doi.org/10.1016/j.fluid.2016.11.009.

(112) Fonseca, F. G.; Funke, A.; Dahmen, N. Aspen Plus^{TM} Modeling of Fractional Condensation Schemes for Production of Fast Pyrolysis Bio-Oil. In *27th European Biomass Conference and Exhibition*; ETA-Florence Renewable Energies: Lisbon, 2019; pp 681–683. https://doi.org/10.5071/27thEUBCE2019-3BV.7.9.

(113) Sui, H.; Yang, H.; Shao, J.; Wang, X.; Li, Y.; Chen, H. Fractional Condensation of Multicomponent Vapors from Pyrolysis of Cotton Stalk. *Energy and Fuels* **2014**, *28* (8), 5095–5102. https://doi.org/10.1021/ef5006012.

(114) Huang, A. N.; Hsu, C. P.; Hou, B. R.; Kuo, H. P. Production and Separation of Rice Husk Pyrolysis Bio-Oils from a Fractional Distillation Column Connected Fluidized Bed Reactor. *Powder Technol* **2018**, *323*, 588–593. https://doi.org/10.1016/j.powtec.2016.03.052.

(115) Yin, R.; Liu, R.; Mei, Y.; Fei, W.; Sun, X. Characterization of Bio-Oil and Bio-Char Obtained from Sweet Sorghum Bagasse Fast Pyrolysis with Fractional Condensers. *Fuel* **2013**, *112*, 96–104. https://doi.org/10.1016/j.fuel.2013.04.090.

(116) Onarheim, K.; Solantausta, Y. Y.; Lehto, J. Process Simulation Development of Fast Pyrolysis of Wood Using Aspen Plus. *Energy & Fuels* **2015**, *29* (1), 205–217. https://doi.org/10.1021/ef502023y.

(117) Krutof, A.; Hawboldt, K. A. Thermodynamic Model of Fast Pyrolysis Bio-Oil Advanced Distillation Curves. *Fuel* **2020**, *261* (July 2019), 116446. https://doi.org/10.1016/j.fuel.2019.116446.

(118) Fonseca, F. G. Process Simulation and Optimization of Biomass Fast Pyrolysis. Ph.D, Karlsruhe Institute of Technology, Karlsruhe, 2023. https://doi.org/10.5445/IR/1000161174.

(119) Bharti, A.; Verma, R.; Prerna; Sarvesh Namdeo; Malviya, A.; Banerjee, T.; Sandler, S. I. Liquid-Liquid Equilibria and COSMO-SAC Modeling of Organic Solvent/Ionic Liquid - Hydroxyacetone - Water Mixtures. *Fluid Phase Equilib* **2018**, *462*, 73–84. https://doi.org/10.1016/j.fluid.2018.01.026.

(120) Cesari, L.; Canabady-Rochelle, L.; Mutelet, F. Separation of Phenols from Lignin Pyrolysis Oil Using Ionic Liquid. *Sep Purif Technol* **2019**, *209*, 528–534. https://doi.org/10.1016/j.seppur.2018.07.083.

(121) Ille, Y.; Sánchez, F. A.; Dahmen, N.; Pereda, S. Multiphase Equilibria Modeling of Fast Pyrolysis Bio-Oils. Group Contribution Associating Equation of State Extension to Lignin Monomers and Derivatives. *Ind Eng Chem Res* **2019**, *58* (17), 7318–7331. https://doi.org/10.1021/acs.iecr.9b00227.

(122) Li, H.; Xia, S.; Wu, M.; Ma, P. Isobaric (Vapour+liquid) Equilibria of Binary Systems Containing Butyl Acetate for the Separation of Methoxy Aromatic Compounds (Anisole and Guaiacol) from Biomass Fast Pyrolysis Oil. *J Chem Thermodyn* **2015**, *87*, 141–146. https://doi.org/10.1016/j.jct.2015.04.003.

(123) Li, X.; Kersten, S. R. A.; Schuur, B. Extraction of Guaiacol from Model Pyrolytic Sugar Stream with Ionic Liquids. *Ind Eng Chem Res* **2016**, *55* (16), 4703–4710. https://doi.org/10.1021/acs.iecr.6b00100.

(124) Prieto, M. G.; Sánchez, F. A.; Pereda, S. A Group Contribution Equation of State for Biorefineries. GCA-EOS Extension to Bioether Fuels and Their Mixtures with n-Alkanes. *J Chem Eng Data* **2019**, *64* (5), 2170–2185. https://doi.org/10.1021/acs.jced.8b01153.

(125) Sánchez, F. A.; Ille, Y.; Dahmen, N.; Pereda, S. GCA-EOS Extension to Mixtures of Phenol Ethers and Derivatives with Hydrocarbons and Water. *Fluid Phase Equilib* **2019**, *490*, 13–21. https://doi.org/10.1016/j.fluid.2019.02.017.

(126) Shang, Q.; Xiao, J.; Li, Y.; Liu, W.; Liu, X.; Cui, G.; Shi, X.; Xia, S.; Tang, B. Isobaric Vapor–Liquid Equilibria of Binary Systems Containing Cyclohexane for the Separation of Phenolic Compounds from Biomass Fast Pyrolysis Oils. *J Chem Eng Data* **2021**, *66* (6), 2374–2382. https://doi.org/10.1021/acs.jced.0c01000.

(127) Stephan, C.; Dicko, M.; Stringari, P.; Coquelet, C. Liquid-Liquid Equilibria of Water + Solutes (Acetic Acid/ Acetol/Furfural/Guaiacol/Methanol/Phenol/Propanal) + Solvents (Isopropyl Acetate/Toluene) Ternary Systems for Pyrolysis Oil Fractionation. *Fluid Phase Equilib* **2018**, *468*, 49–57. https://doi.org/10.1016/j.fluid.2018.04.016.

(128) Papadikis, K.; Gu, S.; Bridgwater, A. V. Eulerian Model for the Condensation of Pyrolysis Vapors in a Water Condenser. *Energy and Fuels* **2011**, *25* (4), 1859–1868. https://doi.org/10.1021/ef200120b.

(129) Jalalinejad, A.; Seyf, J. Y.; Funke, A.; Dahmen, N. Solvent Screening for Separation of Lignin-Derived Molecules Using the NIST-UNIFAC Model. *ACS Sustain Chem Eng* **2023**, *11* (20), 7863–7873. https://doi.org/10.1021/acssuschemeng.3c00906.

(130) Manrique, R.; Terrell, E.; Kostetskyy, P.; Chejne, F.; Olarte, M.; Broadbelt, L.; García-Pérez, M. Elucidating Biomass-Derived Pyrolytic Lignin Structures from Demethylation Reactions through Density Functional Theory Calculations. *Energy and Fuels* **2023**, *37* (7), 5189–5205. https://doi.org/10.1021/acs.energyfuels.2c04292.

(131) Kabir, G.; Hameed, B. H. Recent Progress on Catalytic Pyrolysis of Lignocellulosic Biomass to High-Grade Bio-Oil and Bio-Chemicals. *Renewable and Sustainable Energy Reviews* **2017**, *70* (January), 945–967. https://doi.org/10.1016/j.rser.2016.12.001.

(132) Campos-Franzani, M. I.; Gajardo-Parra, N. F.; Pazo-Carballo, C.; Aravena, P.; Santiago, R.; Palomar, J.; Escalona, N.; Canales, R. I. Extraction of Guaiacol from Hydrocarbons as an Alternative for the Upgraded Bio-Oil Purification: Experimental and

Computational Thermodynamic Study. *Fuel* **2020**, *280*, 118405. https://doi.org/10.1016/j.fuel.2020.118405.

(133) Kougioumtzis, M. A.; Marianou, A.; Atsonios, K.; Michailof, C.; Nikolopoulos, N.; Koukouzas, N.; Triantafyllidis, K.; Lappas, A.; Kakaras, E. Production of 5-HMF from Cellulosic Biomass: Experimental Results and Integrated Process Simulation. *Waste Biomass Valorization* **2018**, *9* (12), 2433–2445. https://doi.org/10.1007/s12649-018-0267-0.

(134) Cesari, L.; Namysl, S.; Canabady-Rochelle, L.; Mutelet, F. Phase Equilibria of Phenolic Compounds in Water or Ethanol. *Fluid Phase Equilib* **2017**, *453*, 58–66. https://doi.org/10.1016/j.fluid.2017.09.008.

(135) Dutta, A.; Sahir, A.; Tan, E.; Humbird, D.; Snowden-Swan, L. J.; Meyer, P.; Ross, J.; Sexton, D.; Yap, R.; Lukas, J. L. *Process Design and Economics for the Conversion of Lignocellulosic Biomass to Hydrocarbon Fuels. Thermochemical Research Pathways with In Situ and Ex Situ Upgrading of Fast Pyrolysis Vapors*; Golden, CO (United States), 2015. https://doi.org/10.2172/1215007.

(136) Mohammed, I. Y.; Abakr, Y. A.; Mokaya, R. Integrated Biomass Thermochemical Conversion for Clean Energy Production: Process Design and Economic Analysis. *J Environ Chem Eng* **2019**, *7* (3), 103093. https://doi.org/10.1016/j.jece.2019.103093.

(137) Feng, W.; Van Der Kooi, H. J.; De Swaan Arons, J. Application of the SAFT Equation of State to Biomass Fast Pyrolysis Liquid. *Chem Eng Sci* **2005**, *60* (3), 617–624. https://doi.org/10.1016/j.ces.2004.08.023.

(138) Mohammed, I. Y.; Abakr, Y. A.; Mokaya, R. Integrated Biomass Thermochemical Conversion for Clean Energy Production: Process Design and Economic Analysis. *J Environ Chem Eng* **2019**, *7* (3), 103093. https://doi.org/10.1016/j.jece.2019.103093.

(139) Fardhyanti, D. S.; Triwibowo, B.; Istanto, H.; Anajib, M. K.; Larasati, A.; Oktaviani, W. Liquid Phase Equilibrium of Phenol Extraction from Bio-Oil Produced by Biomass Pyrolysis Using Thermodynamic Models. *Chin J Chem Eng* **2019**, *27* (2), 391–399. https://doi.org/10.1016/j.cjche.2018.08.011.

(140) Motta, I. L.; Marchesan, A. N.; Guimarães, H. R.; Chagas, M. F.; Bonomi, A.; Maciel, M. R. W.; Filho, R. M. Fast Pyrolysis Simulation via Kinetic Approach and Multivariate Analysis to Assess the Effect of Biomass Properties on Product Yields, Properties, and Pyrolyzer Performance. *Energy Convers Manag* **2023**.

(141) Neves, R. C. Techno-Economic Investigation of First-Generation Sugarcane Biorefinery Integrated with Second Generation Thermochemical Route to Produce Biojet Fuel, Universidade Estadual de Campinas, 2019.

(142) Gorensek, M. B.; Shukre, R.; Chen, C.-C. C. Development of a Thermophysical Properties Model for Flowsheet Simulation of Biomass Pyrolysis Processes. *ACS Sustain Chem Eng* **2019**, *7* (9), 9017–9027. https://doi.org/10.1021/acssuschemeng.9b01278.

(143) Gupta, M.; McFarlan, A.; Preto, F.; Ferguson, M. Comparative Evaluation of a Predictive Process Model for Multistage Condensation in Fast Pyrolysis Systems. In *2020 Thermal and Catalytic Sciences Virtual Symposium*; Cvent: Kennewick, USA, 2020.

(144) Peters, J. F.; Banks, S. W.; Bridgwater, A. V.; Dufour, J. A Kinetic Reaction Model for Biomass Pyrolysis Processes in Aspen Plus. *Appl Energy* **2017**, *188*, 595–603. https://doi.org/10.1016/j.apenergy.2016.12.030.

(145) Gura, L. Development of Pyrolysis Process Models for the Production of Lignin Based Phenols Using Aspen Plus, Stellenbosch University, 2017.

(146) Shahbaz, M.; AlNouss, A.; Parthasarathy, P.; Abdelaal, A. H.; Mackey, H.; McKay, G.; Al-Ansari, T. Investigation of Biomass Components on the Slow Pyrolysis Products Yield Using Aspen Plus for Techno-Economic Analysis. *Biomass Convers Biorefin* **2020**. https://doi.org/10.1007/s13399-020-01040-1.

(147) Shemfe, M. B.; Gu, S.; Ranganathan, P. Techno-Economic Performance Analysis of Biofuel Production and Miniature Electric Power Generation from Biomass Fast Pyrolysis and Bio-Oil Upgrading. *Fuel* **2015**, *143* (March), 361–372. https://doi.org/10.1016/j.fuel.2014.11.078.

(148) Hammer, N. L.; Boateng, A. a; Mullen, C. a; Wheeler, M. C. Aspen Plus®and Economic Modeling of Equine Waste Utilization for Localized Hot Water Heating via Fast Pyrolysis. *J Environ Manage* **2013**, *128*, 594–601. https://doi.org/10.1016/j.jenvman.2013.06.008.

(149) Stephan, C.; Dicko, M.; Stringari, P.; Coquelet, C. Liquid-Liquid Equilibria of Water + Solutes (Acetic Acid/ Acetol/Furfural/Guaiacol/Methanol/Phenol/Propanal) + Solvents (Isopropyl Acetate/Toluene) Ternary Systems for Pyrolysis Oil Fractionation. *Fluid Phase Equilib* **2018**, *468*, 49–57. https://doi.org/10.1016/j.fluid.2018.04.016.

(150) Humbird, D.; Trendewicz, A.; Braun, R.; Dutta, A. One-Dimensional Biomass Fast Pyrolysis Model with Reaction Kinetics Integrated in an Aspen Plus Biorefinery Process Model. *ACS Sustain Chem Eng* **2017**, *5* (3), 2463–2470. https://doi.org/10.1021/acssuschemeng.6b02809.

(151) Wagh, A. S. W. Modelling and Simulation of Biomass Fast Pyrolysis Process: Kinetics, Reactor, and Condenser Systems. Doctor of Philosophy, Curtin University, Perth, 2019.

(152) Wang, H.; Liu, Y.; Gunawan, R.; Zhang, L.; Wang, Z.; Li, C.-Z. Reactions and Distribution of Levoglucosan during the High-Pressure Reactive Distillation of Bio-Oil. *Ind Eng Chem Res* **2021**, *60* (17), 6298–6305. https://doi.org/10.1021/acs.iecr.1c00736.

(153) Fele Žilnik, L.; Jazbinšek, A. Recovery of Renewable Phenolic Fraction from Pyrolysis Oil. *Sep Purif Technol* **2012**, *86*, 157–170. https://doi.org/10.1016/j.seppur.2011.10.040.

(154) Jasperson, L. V.; McDougal, R. J.; Diky, V.; Paulechka, E.; Chirico, R. D.; Kroenlein, K.; Iisa, K.; Dutta, A. Liquid–Liquid Equilibrium Measurements for Model Systems Related to Catalytic Fast Pyrolysis of Biomass. *J Chem Eng Data* **2017**, *62* (1), 243–252. https://doi.org/10.1021/acs.jced.6b00625.

(155) Bridgwater, A. V. Renewable Fuels and Chemicals by Thermal Processing of Biomass. *Chemical Engineering Journal* **2003**, *91* (2–3), 87–102. https://doi.org/10.1016/S1385-8947(02)00142-0.

(156) Garcia-Perez, M.; Lewis, T.; Kruger, C. E. *Methods for Producing Biochar and Advanced Biofuels in Washington State*; 2010. https://doi.org/Ecology Publication Number 11-07-017.

(157) Bridgwater, A. V. V. Review of Fast Pyrolysis of Biomass and Product Upgrading. *Biomass Bioenergy* **2012**, *38*, 68–94. https://doi.org/10.1016/j.biombioe.2011.01.048.

(158) Papari, S.; Hawboldt, K. A Review on Condensing System for Biomass Pyrolysis Process. *Fuel Processing Technology* **2018**, *180* (June), 1–13. https://doi.org/10.1016/j.fuproc.2018.08.001.

(159) Honeywell UOP. *RTP Biomass Conversion - Renewable Fuels*. https://uop.honeywell.com/en/industry-solutions/renewable-fuels/rtp-biomass-conversion (accessed 2021-05-19).

(160) Krutof, A.; Hawboldt, K. A. Upgrading of Biomass Sourced Pyrolysis Oil Review: Focus on Co-Pyrolysis and Vapour Upgrading during Pyrolysis. *Biomass Convers Biorefin* **2018**, *8* (3), 775–787. https://doi.org/10.1007/s13399-018-0326-6.

(161) Elliott, D. C. Historical Developments in Hydroprocessing Bio-Oils. *Energy & Fuels* **2007**, *21* (3), 1792–1815. https://doi.org/10.1021/ef070044u.

(162) Krutof, A.; Hawboldt, K. Blends of Pyrolysis Oil, Petroleum, and Other Bio-Based Fuels: A Review. *Renewable and Sustainable Energy Reviews* **2016**, *59*, 406–419. https://doi.org/10.1016/j.rser.2015.12.304.

(163) Lindfors, C.; Elliott, D. C.; Prins, W.; Oasmaa, A.; Lehtonen, J. Co-Processing of Biocrudes in Oil Refineries. *Energy & Fuels* **2023**, *37* (2), 799–804. https://doi.org/10.1021/acs.energyfuels.2c04238.

(164) Sipilä, K.; Kuoppala, E.; Fagernäs, L.; Oasmaa, A. Characterization of Biomass-Based Flash Pyrolysis Oils. *Biomass Bioenergy* **1998**, *14* (2), 103–113. https://doi.org/10.1016/S0961-9534(97)10024-1.

(165) Karagöz, S. Comments on "Influence of Extraction Solvents on the Recovery Yields and Properties of Bio-Oils from Woody Biomass Liquefaction in Sub-Critical Water, Ethanol or Water–Ethanol Mixed Solvent." *Fuel* **2022**, *319*, 123865. https://doi.org/10.1016/j.fuel.2022.123865.

(166) Olarte, M. V.; Taylor, J.; Swita, M.; Lemmon, T.; Ma, R.; Auberry, D.; Burton, S.; Howe, D.; Padmaperuma, A. Revisiting Quantification of Phenolics in Bio-Oils and Biocrudes. In *2020 Thermal and Catalytic Sciences Virtual Symposium*; Cvent: Kennewick, USA, 2020.

(167) Schmitt, C. C.; Boscagli, C.; Rapp, M.; Raffelt, R.; Dahmen, N.; Raffelt, K.; Dahmen, N.; Conference, E. B. Characterization of Light and Heavy Phase of Pyrolysis-Oil from Distinct Biomass for Further Upgrading Reactions. *European Biomass Conference and Exhibition Proceedings* **2017**, *2017* (June), 12–15. https://doi.org/10.5071/25thEUBCE2017-3AV.3.15.

(168) Lopes, F. J. F.; Silvério, F. O.; Baffa, D. C. F.; Loureiro, M. E.; Barbosa, M. H. P. Determination of Sugarcane Bagasse Lignin S/G/H Ratio by Pyrolysis GC/MS. *Journal of Wood Chemistry and Technology* **2011**, *31* (4), 309–323. https://doi.org/10.1080/02773813.2010.550379.

(169) Banyasz, J. L.; Li, S.; Lyons-Hart, J. L.; Shafer, K. H. Cellulose Pyrolysis: The Kinetics of Hydroxyacetaldehyde Evolution. *J Anal Appl Pyrolysis* **2001**, *57* (2), 223–248. https://doi.org/10.1016/S0165-2370(00)00135-2.

(170) Oh, S.-J.; Choi, G.-G.; Kim, J.-S. Production of Acetic Acid-Rich Bio-Oils from the Fast Pyrolysis of Biomass and Synthesis of Calcium Magnesium Acetate Deicer. *J Anal Appl Pyrolysis* **2017**, *124*, 122–129. https://doi.org/10.1016/j.jaap.2017.01.032.

(171) Shen, D.; Jin, W.; Hu, J.; Xiao, R.; Luo, K. An Overview on Fast Pyrolysis of the Main Constituents in Lignocellulosic Biomass to Valued-Added Chemicals: Structures, Pathways and Interactions. *Renewable and Sustainable Energy Reviews* **2015**, *51*, 761–774. https://doi.org/10.1016/j.rser.2015.06.054.

(172) Azeez, A. M.; Meier, D.; Odermatt, J. Temperature Dependence of Fast Pyrolysis Volatile Products from European and African Biomasses. *J Anal Appl Pyrolysis* **2011**, *90* (2), 81–92. https://doi.org/10.1016/j.jaap.2010.11.005.

(173) Martínez, J. D.; Veses, A.; Mastral, A. M.; Murillo, R.; Navarro, M. V.; Puy, N.; Artigues, A.; Bartrolí, J.; García, T. Co-Pyrolysis of Biomass with Waste Tyres: Upgrading of Liquid Bio-Fuel. *Fuel Processing Technology* **2014**, *119*, 263–271. https://doi.org/10.1016/j.fuproc.2013.11.015.

(174) Bedmutha, R. J.; Ferrante, L.; Briens, C.; Berruti, F.; Inculet, I. Single and Two-Stage Electrostatic Demisters for Biomass Pyrolysis Application. *Chemical Engineering and Processing: Process Intensification* **2009**, *48* (6), 1112–1120. https://doi.org/10.1016/j.cep.2009.02.007.

(175) Gollakota, A. R. K.; Reddy, M.; Subramanyam, M. D.; Kishore, N. A Review on the Upgradation Techniques of Pyrolysis Oil. *Renewable and Sustainable Energy Reviews* **2016**, *58*, 1543–1568. https://doi.org/10.1016/j.rser.2015.12.180.

(176) Lugo-José, Y. K.; Monnier, J. R.; Heyden, A.; Williams, C. T. Hydrodeoxygenation of Propanoic Acid over Silica-Supported Palladium: Effect of Metal Particle Size. *Catal. Sci. Technol.* **2014**, *4* (11), 3909–3916. https://doi.org/10.1039/C4CY00605D.

(177) Hoekstra, E.; Westerhof, R. J. M.; Brilman, W.; Van Swaaij, W. P. M.; Kersten, S. R. A.; Hogendoorn, K. J. A.; Windt, M. Heterogeneous and Homogeneous Reactions of Pyrolysis Vapors from Pine Wood. *AIChE Journal* **2012**, *58* (9), 2830–2842. https://doi.org/10.1002/aic.12799.

(178) Alves, A.; Schwanninger, M.; Pereira, H.; Rodrigues, J. Analytical Pyrolysis as a Direct Method to Determine the Lignin Content in Wood: Part 1: Comparison of Pyrolysis Lignin with Klason Lignin. *J Anal Appl Pyrolysis* **2006**, *76* (1–2), 209–213. https://doi.org/10.1016/j.jaap.2005.11.004.

(179) Wang, R.; Ben, H. Accelerated Aging Process of Bio-Oil Model Compounds: A Mechanism Study. *Front Energy Res* **2020**, *8*. https://doi.org/10.3389/fenrg.2020.00079.

(180) Diebold, J. P. P. *A Review of the Chemical and Physical Mechanisms of the Storage Stability of Fast Pyrolysis Bio-Oils*; Lakewood, CO, USA, 2000. https://doi.org/NREL/SR-570-27613.

(181) Cai, J.; Rahman, Md. M.; Zhang, S.; Sarker, M.; Zhang, X.; Zhang, Y.; Yu, X.; Fini, E. H. Review on Aging of Bio-Oil from Biomass Pyrolysis and Strategy to Slowing Aging. *Energy & Fuels* **2021**, *35* (15), 11665–11692. https://doi.org/10.1021/acs.energyfuels.1c01214.

(182) Xiong, W.; Fu, Y.; 郭庆祥; QingXiang Lu, Q. & G. Aging Behavior and Mechanism of Bio-Oil. *Chinese Science Bulletin* **2009**, *54* (15), 2188–2195. https://doi.org/10.1360/972009-50.

(183) Wu, L.; Hu, X.; Wang, S.; Mourant, D.; Song, Y.; Li, T.; Li, C.-Z. Formation of Coke during the Esterification of Pyrolysis Bio-Oil. *RSC Adv* **2016**, *6* (89), 86485–86493. https://doi.org/10.1039/C6RA14939A.

(184) Routray, K.; Barnett, K. J.; Huber, G. W. Hydrodeoxygenation of Pyrolysis Oils. *Energy Technology* **2017**, *5* (1), 80–93. https://doi.org/10.1002/ente.201600084.

(185) del Río, J. C.; Lino, A. G.; Colodette, J. L.; Lima, C. F.; Gutiérrez, A.; Martínez, Á. T.; Lu, F.; Ralph, J.; Rencoret, J. Differences in the Chemical Structure of the Lignins from Sugarcane Bagasse and Straw. *Biomass Bioenergy* **2015**, *81*, 322–338. https://doi.org/10.1016/j.biombioe.2015.07.006.

(186) Lin, X.; Sui, S.; Tan, S.; Pittman, C.; Sun, J.; Zhang, Z. Fast Pyrolysis of Four Lignins from Different Isolation Processes Using Py-GC/MS. *Energies (Basel)* **2015**, *8* (6), 5107–5121. https://doi.org/10.3390/en8065107.

(187) Lupoi, J. S.; Singh, S.; Parthasarathi, R.; Simmons, B. A.; Henry, R. J. Recent Innovations in Analytical Methods for the Qualitative and Quantitative Assessment of Lignin. *Renewable and Sustainable Energy Reviews* **2015**, *49*, 871–906. https://doi.org/10.1016/j.rser.2015.04.091.

(188) Lyu, G.; Wu, S.; Zhang, H. Estimation and Comparison of Bio-Oil Components from Different Pyrolysis Conditions. *Front Energy Res* **2015**, *3*. https://doi.org/10.3389/fenrg.2015.00028.

(189) Chen, T.; Deng, C.; Liu, R. Effect of Selective Condensation on the Characterization of Bio-Oil from Pine Sawdust Fast Pyrolysis Using a Fluidized-Bed Reactor. *Energy and Fuels* **2010**, *24* (12), 6616–6623. https://doi.org/10.1021/ef1011963.

(190) yang, Q.; Wu, S.; Lou, R.; Lv, G. Analysis of Wheat Straw Lignin by Thermogravimetry and Pyrolysis-Gas Chromatography/Mass Spectrometry. *J Anal Appl Pyrolysis* **2010**, *87* (1), 65–69. https://doi.org/10.1016/j.jaap.2009.10.006.

(191) Adolf, K. Entwicklung Einer Thermodynamischen Siedekurve von Schwelwasser. BSc, Karlsruher Institut für Technologie (KIT), 2021.

(192) Westerhof, R. J. M.; Kuipers, N. J. M.; Kersten, S. R. A.; van Swaaij, W. P. M. Controlling the Water Content of Biomass Fast Pyrolysis Oil. *Ind Eng Chem Res* **2007**, *46* (26), 9238–9247. https://doi.org/10.1021/ie070684k.

(193) Jones, S.; Meyer, P.; Snowden-Swan, L.; Susanne, K. J.; Pimphan, M.; Snowden-SwanLesley; Asanga, P.; Eric, T.; Abhijit, D.; Jacob, J.; Cafferty; Jones, S.; Meyer, P.; Snowden-Swan, L. Process Design and Economics for the Conversion of Lignocellulosic Biomass to Hydrocarbon Fuels: Fast Pyrolysis and Hydrotreating Bio-Oil Pathway. *Energy* **2013**, No. November, 97. https://doi.org/PNNL - 23053 NREL/TP - 5100 - 61178.

(194) Wooley, R. J.; Putsche, V. *Development of an ASPEN PLUS Physical Property Database for Biofuels Components*; Golden, Colorado, 1996. https://doi.org/10.2172/257362.

(195) Li, H.; Xia, S.; Ma, P.; Yan, F.; Yang, Z.; Li, Y. Isobaric (Vapour+liquid) Equilibria for Three Binary Systems (Toluene+anisole, n-Butylbenzene+anisole, and Guaiacol+anisole) at 101.33kPa. *Fluid Phase Equilib* **2014**, *369*, 109–114. https://doi.org/10.1016/j.fluid.2014.02.025.

(196) Clair, J. M. St.; Spencer, K. M.; Beaver, M. R.; Crounse, J. D.; Paulot, F.; Wennberg, P. O. Quantification of Hydroxyacetone and Glycolaldehyde Using Chemical Ionization Mass Spectrometry. *Atmos Chem Phys* **2014**, *14* (8), 4251–4262. https://doi.org/10.5194/acp-14-4251-2014.

(197) Pereira da Silva Maciel, G.; Machado, M. E.; Barbará, J. A.; Molin, D. D.; Caramão, E. B.; Jacques, R. A. GC × GC/TOFMS Analysis Concerning the Identification of Organic Compounds Extracted from the Aqueous Phase of Sugarcane Straw Fast Pyrolysis Oil. *Biomass Bioenergy* **2016**, *85*, 198–206. https://doi.org/10.1016/j.biombioe.2015.11.009.

(198) Al-Owaisi, M.; Al-Hadiwi, N.; Khan, S. A. GC-MS Analysis, Determination of Total Phenolics, Flavonoid Content and Free Radical Scavenging Activities of Various Crude Extracts of Moringa Peregrina (Forssk.) Fiori Leaves. *Asian Pac J Trop Biomed* **2014**, *4* (12), 964–970. https://doi.org/10.12980/APJTB.4.201414B295.

(199) Gupta, M.; Bronson, B.; Mazerolle, D.; Ferguson, M.; Preto, F. Evaluating Stability of Chemically Quenched Pyrolysis Vapours Using Accelerated Aging Tests. In *2020 Thermal and Catalytic Sciences Virtual Symposium*; Cvent: Kennewick, USA, 2020.

(200) Lehto, J.; Oasmaa, A.; Solantausta, Y.; Kytö, M.; Chiaramonti, D. Fuel Oil Quality and Combustion of Fast Pyrolysis Bio-Oils. *VTT Publications* **2013**, No. 87, 79. https://doi.org/http://dx.doi.org/10.1016/j.apenergy.2013.11.040.

(201) Stark, Y. H. Modellierung Der Kondensation von Schnellpyrolysedämpfen Unter Berücksichtigung von Aerosolbildung, Karlsruher Instituts für Technologie, 2020.

(202) Shoji, T.; Kawamoto, H.; Saka, S. Boiling Point of Levoglucosan and Devolatilization Temperatures in Cellulose Pyrolysis Measured at Different Heating Area Temperatures. *J Anal Appl Pyrolysis* **2014**, *109*, 185–195. https://doi.org/10.1016/j.jaap.2014.06.014.

(203) Ranzi, E.; Cuoci, A.; Faravelli, T.; Frassoldati, A.; Migliavacca, G.; Pierucci, S.; Sommariva, S. Chemical Kinetics of Biomass Pyrolysis. *Energ Fuel* **2008**, *22* (6), 4292–4300. https://doi.org/10.1021/ef800551t.

(204) Corbetta, M.; Pierucci, S.; Ranzi, E.; Bennadji, H.; Fisher, E. M. Multistep Kinetic Model of Biomass Pyrolysis. In *XXXVI Meeting of the Italian Section of the Combustion Institute*; 2013; pp 4–9.

(205) Anca-Couce, A.; Sommersacher, P.; Scharler, R. Online Experiments and Modelling with a Detailed Reaction Scheme of Single Particle Biomass Pyrolysis. *J Anal Appl Pyrolysis* **2017**, *127*, 411–425. https://doi.org/10.1016/j.jaap.2017.07.008.

(206) Trendewicz, A.; Evans, R.; Dutta, A.; Sykes, R.; Carpenter, D.; Braun, R. Evaluating the Effect of Potassium on Cellulose Pyrolysis Reaction Kinetics. *Biomass Bioenergy* **2015**, *74*, 15–25. https://doi.org/10.1016/j.biombioe.2015.01.001.

(207) Ranzi, E.; Debiagi, P. E. A.; Frassoldati, A. Mathematical Modeling of Fast Biomass Pyrolysis and Bio-Oil Formation. Note I: Kinetic Mechanism of Biomass Pyrolysis. *ACS Sustain Chem Eng* **2017**, *5* (4), 2867–2881. https://doi.org/10.1021/acssuschemeng.6b03096.

(208) Ranzi, E.; Debiagi, P. E. A.; Frassoldati, A. Mathematical Modeling of Fast Biomass Pyrolysis and Bio-Oil Formation. Note II: Secondary Gas-Phase Reactions and Bio-Oil Formation. *ACS Sustain Chem Eng* **2017**, *5* (4), 2882–2896. https://doi.org/10.1021/acssuschemeng.6b03098.

(209) Faravelli, T.; Frassoldati, A.; Migliavacca, G.; Ranzi, E. Detailed Kinetic Modeling of the Thermal Degradation of Lignins. *Biomass Bioenergy* **2010**, *34* (3), 290–301. https://doi.org/10.1016/j.biombioe.2009.10.018.

(210) Elliott, D. C.; Meier, D.; Oasmaa, A.; Van De Beld, B.; Bridgwater, A. V.; Marklund, M. Results of the International Energy Agency Round Robin on Fast Pyrolysis Bio-Oil Production. *Energy and Fuels* **2017**, *31* (5), 5111–5119. https://doi.org/10.1021/acs.energyfuels.6b03502.

(211) Czernik, S.; Johnson, D. K.; Black, S. Stability of Wood Fast Pyrolysis Oil. *Biomass Bioenergy* **1994**, *7* (1–6), 187–192. https://doi.org/10.1016/0961-9534(94)00058-2.

(212) Debiagi, P.; Gentile, G.; Cuoci, A.; Frassoldati, A.; Ranzi, E.; Faravelli, T. A Predictive Model of Biochar Formation and Characterization. *J Anal Appl Pyrolysis* **2018**, *134*, 326–335. https://doi.org/10.1016/j.jaap.2018.06.022.

(213) Scholze, B.; Hanser, C.; Meier, D. Characterization of the Water-Insoluble Fraction from Fast Pyrolysis Liquids (Pyrolytic Lignin): Part II. GPC, Carbonyl Goups, and 13C-NMR. *J Anal Appl Pyrolysis* **2001**, *58–59*, 387–400. https://doi.org/10.1016/S0165-2370(00)00173-X.

(214) Bayerbach, R.; Nguyen, V. D.; Schurr, U.; Meier, D. Characterization of the Water-Insoluble Fraction from Fast Pyrolysis Liquids (Pyrolytic Lignin). Part III. Molar Mass Characteristics by SEC, MALDI-TOF-MS, LDI-TOF-MS, and Py-FIMS. *J Anal Appl Pyrolysis* **2006**, *77* (2), 95–101. https://doi.org/10.1016/j.jaap.2006.02.002.

(215) Bayerbach, R.; Meier, D. Characterization of the Water-Insoluble Fraction from Fast Pyrolysis Liquids (Pyrolytic Lignin). Part IV: Structure Elucidation of Oligomeric Molecules. *J Anal Appl Pyrolysis* **2009**, *85* (1–2), 98–107. https://doi.org/10.1016/j.jaap.2008.10.021.

(216) Kröhl, F. Berechnung Der Aktivitätskoefizienten Einer Modellmischung Fur Pyrolyseöle Mittels Gruppenbeitragsmethoden. Bachelorarbeit, Karlsruhe Institute für Technologie, 2015.

(217) Fonts, I.; Atienza-Martínez, M.; Carstensen, H.-H. H.; Benés, M.; Pinheiro Pires, A. P.; Garcia-Perez, M.; Bilbao, R. Thermodynamic and Physical Property Estimation of Compounds Derived from the Fast Pyrolysis of Lignocellulosic Materials. *Energy & Fuels* **2021**, *35* (21), 17114–17137. https://doi.org/10.1021/acs.energyfuels.1c01709.

(218) Dearden, J. C. Quantitative Structure-Property Relationships for Prediction of Boiling Point, Vapor Pressure, and Melting Point. *Environ Toxicol Chem* **2003**, *22* (8), 1696. https://doi.org/10.1897/01-363.

(219) Mackay, D.; Shiu, W.-Y.; Ma, K.-C.; Lee, S. C.; Shiu, W.-Y.; Lee, S. C. *Handbook of Physical-Chemical Properties and Environmental Fate for Organic Chemicals*; CRC Press, 2006; Vol. III. https://doi.org/10.1201/9781420044393.

(220) Joback, K. G. Obtain the Best Physical Property Data. *Chem Eng Prog* **2009**, *105* (5), 30–39.

(221) Benson, S. W. New Methods for Estimating the Heats of Formation, Heat Capacities, and Entropies of Liquids and Gases. *J Phys Chem A* **1999**, *103* (51), 11481–11485. https://doi.org/10.1021/jp992971a.

(222) Nesterov, V.; Wieser, M.; Roth, V. 3DMolNet: A Generative Network for Molecular Structures. *arXiv: Biomolecules (q-bio.BM)* **2020**.

(223) Huang, B.; von Lilienfeld, O. A. Ab Initio Machine Learning in Chemical Compound Space. *Chem Rev* **2021**, *121* (16), 10001–10036. https://doi.org/10.1021/acs.chemrev.0c01303.

(224) Plehiers, P. P.; Lengyel, I.; West, D. H.; Marin, G. B.; Stevens, C. V.; Van Geem, K. M. Fast Estimation of Standard Enthalpy of Formation with Chemical Accuracy by Artificial Neural Network Correction of Low-Level-of-Theory Ab Initio Calculations. *Chemical Engineering Journal* **2021**, *426*, 131304. https://doi.org/10.1016/j.cej.2021.131304.

(225) Simmie, J. M.; Somers, K. P. Benchmarking Compound Methods (CBS-QB3, CBS-APNO, G3, G4, W1BD) against the Active Thermochemical Tables: A Litmus Test for Cost-Effective Molecular Formation Enthalpies. *J Phys Chem A* **2015**, *119* (28), 7235–7246. https://doi.org/10.1021/jp511403a.

(226) Marino, D. J. Variability in Physical Constant Parameter Values from Standard Data Sources and the Implication of This Variability for Risk Analysis. *Risk Analysis* **2006**, *26* (2), 555–572. https://doi.org/10.1111/j.1539-6924.2006.00752.x.

(227) Gani, R.; Kontogeorgis, G. M. Chapter 13: Property Models in Computation of Phase Equilibria. In *Computer Aided Chemical Engineering*; Elsevier, 2004; Vol. 19, pp 309–337. https://doi.org/10.1016/S1570-7946(04)80015-4.

(228) Rowley, R. L.; Wilding, W. V.; Oscarson, J. L.; Yang, Y. Database Tools for Evaluating Thermophysical Property Data. *Int J Thermophys* **2007**, *28* (3), 805–823. https://doi.org/10.1007/s10765-007-0235-6.

(229) Joback, K. G.; Reid, R. C. Estimation of Pure-Component Properties from Group-Contributions. *Chem Eng Commun* **1987**, *57* (1–6), 233–243. https://doi.org/10.1080/00986448708960487.

(230) Constantinou, L.; Gani, R. New Group Contribution Method for Estimating Properties of Pure Compounds. *AIChE Journal* **1994**, *40* (10), 1697–1710. https://doi.org/10.1002/aic.690401011.

(231) Cordes, W.; Rarey, J. A New Method for the Estimation of the Normal Boiling Point of Non-Electrolyte Organic Compounds. *Fluid Phase Equilib* **2002**, *201* (2), 409–433. https://doi.org/10.1016/S0378-3812(02)00050-X.

(232) Satou, M.; Itoh, D.; Hattori, H.; Yoshida, T. Evaluation of Ring Size Distribution in a Heavy Oil Based on Boiling Point and Molecular Weight Distributions. *Fuel* **2000**, *79* (3–4), 339–348. https://doi.org/10.1016/S0016-2361(99)00168-4.

(233) Stein, S. E.; Brown, R. L. Estimation of Normal Boiling Points from Group Contributions. *J Chem Inf Comput Sci* **1994**, *34* (3), 581–587. https://doi.org/10.1021/ci00019a016.

(234) Marrero, J.; Gani, R. Group-Contribution Based Estimation of Pure Component Properties. *Fluid Phase Equilib* **2001**, *183–184*, 183–208. https://doi.org/10.1016/S0378-3812(01)00431-9.

(235) Marrero-Morejón, J.; Pardillo-Fontdevila, E. Estimation of Pure Compound Properties Using Group-Interaction Contributions. *AIChE Journal* **1999**, *45* (3), 615–621. https://doi.org/10.1002/aic.690450318.

(236) Twu, C. H. An Internally Consistent Correlation for Predicting the Critical Properties and Molecular Weights of Petroleum and Coal-Tar Liquids. *Fluid Phase Equilib* **1984**, *16* (2), 137–150. https://doi.org/10.1016/0378-3812(84)85027-X.

(237) Lydersen, A. L. *Estimation of Critical Properties of Organic Compounds*; Madison, Wisconsin, 1955.

(238) Fedors, R. F. A Relationship between Chemical Structure and the Critical Temperature. *Chem Eng Commun* **1982**, *16* (1–6), 149–151. https://doi.org/10.1080/00986448208911092.

(239) Ambrose, D. *Correlation and Estimation of Vapor-Liquid Critical Properties: I. Critical Temperatures of Organic Compounds*; Teddington, 1978; Vol. 92.

(240) Klincewicz, K. M.; Reid, R. C. Estimation of Critical Properties with Group Contribution Methods. *AIChE Journal* **1984**, *30* (1), 137–142. https://doi.org/10.1002/aic.690300119.

(241) Nannoolal, Y.; Rarey, J.; Ramjugernath, D. Estimation of Pure Component Properties: Part 2. Estimation of Critical Property Data by Group Contribution. *Fluid Phase Equilib* **2007**, *252* (1–2), 1–27. https://doi.org/10.1016/j.fluid.2006.11.014.

(242) Hogge, J. W.; Giles, N. F.; Knotts, T. A.; Rowley, R. L.; Wilding, W. V. The Riedel Vapor Pressure Correlation and Multi-Property Optimization. *Fluid Phase Equilib* **2016**, *429*, 149–165. https://doi.org/10.1016/j.fluid.2016.08.032.

(243) Lee, B. I.; Kesler, M. G. A Generalized Thermodynamic Correlation Based on Three-Parameter Corresponding States. *AIChE Journal* **1975**, *21* (3), 510–527. https://doi.org/10.1002/aic.690210313.

(244) Harrison, B. K.; Seaton, W. H. Solution to Missing Group Problem for Estimation of Ideal Gas Heat Capacities. *Ind Eng Chem Res* **1988**, *27* (8), 1536–1540. https://doi.org/10.1021/ie00080a031.

(245) Aly, F. A.; Lee, L. L. Self-Consistent Equations for Calculating the Ideal Gas Heat Capacity, Enthalpy, and Entropy. *Fluid Phase Equilib* **1981**, *6* (3–4), 169–179. https://doi.org/10.1016/0378-3812(81)85002-9.

(246) Růžička, V.; Domalski, E. S. Estimation of the Heat Capacities of Organic Liquids as a Function of Temperature Using Group Additivity. II. Compounds of Carbon, Hydrogen, Halogens, Nitrogen, Oxygen, and Sulfur. *J Phys Chem Ref Data* **1993**, *22* (3), 619–657. https://doi.org/10.1063/1.555924.

(247) Růžička, V.; Domalski, E. S. Estimation of the Heat Capacities of Organic Liquids as a Function of Temperature Using Group Additivity. I. Hydrocarbon Compounds. *J Phys Chem Ref Data* **1993**, *22* (3), 597–618. https://doi.org/10.1063/1.555923.

(248) Zábranský, M.; Růžička, V. Estimation of the Heat Capacities of Organic Liquids as a Function of Temperature Using Group Additivity: An Amendment. *J Phys Chem Ref Data* **2004**, *33* (4), 1071–1081. https://doi.org/10.1063/1.1797811.

(249) Chueh, C. F.; Swanson, A. C. Estimation of Liquid Heat Capacity. *Can J Chem Eng* **1973**, *51* (5), 596–600. https://doi.org/10.1002/cjce.5450510511.

(250) Li, P.; Ma, P.-S.; Yi, S.-Z.; Zhao, Z.-G.; Cong, L.-Z. A New Corresponding-States Group-Contribution Method (CSGC) for Estimating Vapor Pressures of Pure Compounds. *Fluid Phase Equilib* **1994**, *101*, 101–119. https://doi.org/10.1016/0378-3812(94)02607-6.

(251) Nannoolal, Y.; Rarey, J.; Ramjugernath, D. Estimation of Pure Component Properties: Part 3. Estimation of the Vapor Pressure of Non-Electrolyte Organic Compounds via Group Contributions and Group Interactions. *Fluid Phase Equilib* **2008**, *269* (1–2), 117–133. https://doi.org/10.1016/j.fluid.2008.04.020.

(252) Simmons, K. A. A Simple Structure-Based Calculator for Estimating Vapor Pressure. *J Agric Food Chem* **1999**, *47* (4), 1711–1716. https://doi.org/10.1021/jf980922+.

(253) Yair, O. Ben; Fredenslund, A. Extension of the UNIFAC Group-Contribution Method for the Prediction of Pure-Component Vapor Pressures. *Industrial & Engineering Chemistry Process Design and Development* **1983**, *22* (3), 433–436. https://doi.org/10.1021/i200022a015.

(254) Ceriani, R.; Meirelles, A. J. A. Predicting Vapor–Liquid Equilibria of Fatty Systems. *Fluid Phase Equilib* **2004**, *215* (2), 227–236. https://doi.org/10.1016/j.fluid.2003.08.011.

(255) Riedel, L. Eine Neue Dampfdruckformel. *Chem. Ing. Tech.* **1954**, No. 26, 83.89.

(256) Mackay, Donald.; Bobra, Alice.; Chan, D. W.; Shiu, W. Ying. Vapor-Pressure Correlations for Low-Volatility Environmental Chemicals. *Environ Sci Technol* **1982**, *16* (10), 645–649. https://doi.org/10.1021/es00104a004.

(257) Mishra, D. S.; Yalkowsky, S. H. Estimation of Vapor Pressure of Some Organic Compounds. *Ind Eng Chem Res* **1991**, *30* (7), 1609–1612. https://doi.org/10.1021/ie00055a029.

(258) Myrdal, P. B.; Yalkowsky, S. H. Estimating Pure Component Vapor Pressures of Complex Organic Molecules. *Ind Eng Chem Res* **1997**, *36* (6), 2494–2499. https://doi.org/10.1021/ie950242l.

(259) Vetere, A. New Correlations for Predicting Vaporization Enthalpies of Pure Compounds. *The Chemical Engineering Journal* **1979**, *17* (2), 157–162. https://doi.org/10.1016/0300-9467(79)85008-X.

(260) Kikic, I.; Vetere, A. Evaluation of Several Literature Equations to Predict the Vaporization Enthalpies at the Normal Boiling Point. *Fluid Phase Equilib* **2011**. https://doi.org/10.1016/j.fluid.2011.06.026.

(261) Ducros, M.; Gruson, J. F.; Sannier, H. Estimation Des Enthalpies de Vaporisation Des Composes Organiques Liquides. Partie 1. Applications Aux Alcanes, Cycloalcanes, Alcenes, Hydrocarbures Benzeniques, Alcools, Alcanes Thiols, Chloro et Bromoalcanes,

Nitriles, Esters, Acides et Aldehydes. *Thermochim Acta* **1980**, *36* (1), 39–65. https://doi.org/10.1016/0040-6031(80)80109-2.

(262) Ducros, M.; Gruson, J. F.; Sannier, H.; Velasco, I. Estimation Des Enthalpies de Vaporisation Des Composes Organiques Liquides. Partie 2. Applications Aux Ethersoxydes, Thioalcanes, Cetones et Amines. *Thermochim Acta* **1981**, *44* (2), 131–140. https://doi.org/10.1016/0040-6031(81)80035-4.

(263) Ducros, M.; Sannier, H. Estimation Des Enthalpies de Vaporisation Des Composes Organiques Liquides, Partie 3. Application Aux Hydrocarbures Insatures. *Thermochim Acta* **1982**, *54* (1–2), 153–157. https://doi.org/10.1016/0040-6031(82)85074-0.

(264) Watson, K. M. Thermodynamics of the Liquid State. *Ind Eng Chem* **1943**, *35* (4), 398–406. https://doi.org/10.1021/ie50400a004.

(265) Reid, R. C.; Prausnitz, J. M.; Sherwood, T. K. *The Properties of Gases and Liquids*; McGraw-Hill: New York, 1977.

(266) Gunn, R. D.; Yamada, T. A Corresponding States Correlation of Saturated Liquid Volumes. *AIChE Journal* **1971**, *17* (6), 1341–1345. https://doi.org/10.1002/aic.690170613.

(267) Yamada, T.; Gunn, R. D. Saturated Liquid Molar Volumes. The Rackett Equation. *J Chem Eng Data* **1973**, *18* (2), 234–236. https://doi.org/10.1021/je60057a006.

(268) Spencer, C. F.; Danner, R. P. Improved Equation for Prediction of Saturated Liquid Density. *J Chem Eng Data* **1972**, *17* (2), 236–241. https://doi.org/10.1021/je60053a012.

(269) Hankinson, R. W.; Thomson, G. H. A New Correlation for Saturated Densities of Liquids and Their Mixtures. *AIChE Journal* **1979**, *25* (4), 653–663. https://doi.org/10.1002/aic.690250412.

(270) Thomson, G. H.; Brobst, K. R.; Hankinson, R. W. An Improved Correlation for Densities of Compressed Liquids and Liquid Mixtures. *AIChE Journal* **1982**, *28* (4), 671–676. https://doi.org/10.1002/aic.690280420.

(271) Honarmand, M.; Haghighat Nezhad, M. R.; Pourgharib, V.; Beigi, M. An Accurate Correlation to Estimate Saturated Molar Volume of Liquids. *Physical Chemistry Research* **2016**, *4* (3), 479–488. https://doi.org/10.22036/pcr.2016.14992.

(272) Reichenberg, D. New Methods for the Estimation of the Viscosity Coefficients of Pure Gases at Moderate Pressures(with Particular Reference to Organic Vapors). *AIChE Journal* **1975**, *21* (1), 181–183. https://doi.org/10.1002/aic.690210130.

(273) Chung, T. H.; Ajlan, M.; Lee, L. L.; Starling, K. E. Generalized Multiparameter Correlation for Nonpolar and Polar Fluid Transport Properties. *Ind Eng Chem Res* **1988**, *27* (4), 671–679. https://doi.org/10.1021/ie00076a024.

(274) Letsou, A.; Stiel, L. I. Viscosity of Saturated Nonpolar Liquids at Elevated Pressures. *AIChE Journal* **1973**, *19* (2), 409–411. https://doi.org/10.1002/aic.690190241.

(275) Poling, B. E.; Prausnitz, J. M.; O’Connell, J. P. Viscosity. In *The Properties of Gases and Liquids*; McGraw-Hill, 2001. https://doi.org/10.1036/0070116822.

(276) Nannoolal, Y.; Rarey, J.; Ramjugernath, D. Estimation of Pure Component Properties. Part 4: Estimation of the Saturated Liquid Viscosity of Non-Electrolyte Organic Compounds via Group Contributions and Group Interactions. *Fluid Phase Equilib* **2009**, *281* (2), 97–119. https://doi.org/10.1016/j.fluid.2009.02.016.

(277) Sastri, S. R. S.; Rao, K. K. A New Temperature–Thermal Conductivity Relationship for Predicting Saturated Liquid Thermal Conductivity. *Chemical Engineering Journal* **1999**, *74* (3), 161–169. https://doi.org/10.1016/S1385-8947(99)00046-7.

(278) Nagvekar, M.; Daubert, T. E. A Group Contribution Method for Liquid Thermal Conductivity. *Ind Eng Chem Res* **1987**, *26* (7), 1362–1365. https://doi.org/10.1021/ie00067a017.

(279) Scheffy, W. J.; Johnson, E. F. Thermal Conductivities of Liquids at High Temperatures. *J Chem Eng Data* **1961**, *6* (2), 245–249. https://doi.org/10.1021/je60010a019.

(280) Lakshmi, D. S.; Prasad, D. H. L. A Rapid Estimation Method for Thermal Conductivity of Pure Liquids. *The Chemical Engineering Journal* **1992**, *48* (3), 211–214. https://doi.org/10.1016/0300-9467(92)80037-B.

(281) Gharagheizi, F.; Ilani-Kashkouli, P.; Sattari, M.; Mohammadi, A. H.; Ramjugernath, D.; Richon, D. Development of a General Model for Determination of Thermal Conductivity of Liquid Chemical Compounds at Atmospheric Pressure. *AIChE Journal* **2013**, *59* (5), 1702–1708. https://doi.org/10.1002/aic.13938.

(282) Brock, J. R.; Bird, R. B. Surface Tension and the Principle of Corresponding States. *AIChE Journal* **1955**, *1* (2), 174–177. https://doi.org/10.1002/aic.690010208.

(283) Macleod, D. B. On a Relation between Surface Tension and Density. *Transactions of the Faraday Society* **1923**, *19* (July), 38. https://doi.org/10.1039/tf9231900038.

(284) Sugden, S. CXLII.—A Relation between Surface Tension, Density, and Chemical Composition. *J. Chem. Soc., Trans.* **1924**, *125* (0), 1177–1189. https://doi.org/10.1039/CT9242501177.

(285) Zuo, Y.-X.; Stenby, E. H. Calculation of Surface Tensions of Polar Mixtures with a Simplified Gradient Theory Model. *Journal of Chemical Engineering of Japan* **1996**, *29* (1), 159–165. https://doi.org/10.1252/jcej.29.159.

(286) Sastri, S. R. S.; Rao, K. K. A Simple Method to Predict Surface Tension of Organic Liquids. *The Chemical Engineering Journal and the Biochemical Engineering Journal* **1995**, *59* (2), 181–186. https://doi.org/10.1016/0923-0467(94)02946-6.

(287) Hakim, D. I.; Steinberg, D.; Stiel, L. I. Generalized Relationship for the Surface Tension of Polar Fluids. *Industrial & Engineering Chemistry Fundamentals* **1971**, *10* (1), 174–175. https://doi.org/10.1021/i160037a032.

(288) Miqueu, C.; Broseta, D.; Satherley, J.; Mendiboure, B.; Lachaise, J.; Graciaa, A. An Extended Scaled Equation for the Temperature Dependence of the Surface Tension of Pure Compounds Inferred from an Analysis of Experimental Data. *Fluid Phase Equilib* **2000**, *172* (2), 169–182. https://doi.org/10.1016/S0378-3812(00)00384-8.

(289) Lapuerta, M.; Hernández, J. P.; Agudelo, J. R. An Equation for the Estimation of Alcohol-Air Diffusion Coefficients for Modelling Evaporation Losses in Fuel Systems.

Appl Therm Eng **2014**, *73* (1), 539–548. https://doi.org/10.1016/j.applthermaleng.2014.08.009.

(290) Slattery, J. C.; Bird, R. B. Calculation of the Diffusion Coefficient of Dilute Gases and of the Self-diffusion Coefficient of Dense Gases. *AIChE Journal* **1958**, *4* (2), 137–142. https://doi.org/10.1002/aic.690040205.

(291) Elliott, R. W.; Watts, H. Diffusion of Some Hydrocarbons in Air: A Regularity in the Diffusion Coefficients of a Homologous Series. *Can J Chem* **1972**, *50* (1), 31–34. https://doi.org/10.1139/v72-005.

(292) Wilke, C. R.; Chang, P. Correlation of Diffusion Coefficients in Dilute Solutions. *AIChE Journal* **1955**, *1* (2), 264–270. https://doi.org/10.1002/aic.690010222.

(293) Miyabe, K.; Isogai, R. Estimation of Molecular Diffusivity in Liquid Phase Systems by the Wilke–Chang Equation. *J Chromatogr A* **2011**, *1218* (38), 6639–6645. https://doi.org/10.1016/j.chroma.2011.07.018.

(294) Stefanis, E.; Panayiotou, C. Prediction of Hansen Solubility Parameters with a New Group-Contribution Method. *Int J Thermophys* **2008**, *29* (2), 568–585. https://doi.org/10.1007/s10765-008-0415-z.

(295) Klopman, G.; Li, J.-Y.; Wang, S.; Dimayuga, M. Computer Automated Log P Calculations Based on an Extended Group Contribution Approach. *J Chem Inf Comput Sci* **1994**, *34* (4), 752–781. https://doi.org/10.1021/ci00020a009.

(296) Sugden, S. CXLI.—The Influence of the Orientation of Surface Molecules on the Surface Tension of Pure Liquids. *J. Chem. Soc., Trans.* **1924**, *125* (0), 1167–1177. https://doi.org/10.1039/CT9242501167.

(297) Mumford, S. A.; Phillips, J. W. C. CCLXXIV.—The Evaluation and Interpretation of Parachors. *J. Chem. Soc.* **1929**, *0* (0), 2112–2133. https://doi.org/10.1039/JR9290002112.

(298) Quayle, O. R. The Parachors of Organic Compounds. An Interpretation and Catalogue. *Chem Rev* **1953**, *53* (3), 439–589. https://doi.org/10.1021/cr60166a003.

(299) Hugill, J. A.; van Welsenes, A. J. Surface Tension: A Simple Correlation for Natural Gas + Conensate Systems. *Fluid Phase Equilib* **1986**, *29*, 383–390. https://doi.org/10.1016/0378-3812(86)85038-5.

(300) Vesovic, V. Prediction of the Thermal Conductivity of Gas Mixtures at Low Pressures. *Int J Thermophys* **2001**, *22* (3), 801–828. https://doi.org/10.1023/A:1010727016194.

(301) Focke, W. W. Correlating Thermal-Conductivity Data for Ternary Liquid Mixtures. *Int J Thermophys* **2008**, *29* (4), 1342–1360. https://doi.org/10.1007/s10765-008-0465-2.

(302) Yoon, P.; Thodos, G. Viscosity of Nonpolar Gaseous Mixtures at Normal Pressures. *AIChE Journal* **1970**, *16* (2), 300–304. https://doi.org/10.1002/aic.690160225.

(303) Yorizane, M.; Yoshimura, S.; Masuoka, H.; Yoshida, H. Thermal Conductivities of Binary Gas Mixtures at High Pressures: Nitrogen-Oxygen, Nitrogen-Argon, Carbon Dioxide-Argon, and Carbon Dioxide-Methane. *Industrial & Engineering Chemistry Fundamentals* **1983**, *22* (4), 458–463. https://doi.org/10.1021/i100012a018.

(304) Chung, T. H.; Lee, L. L.; Starling, K. E. Applications of Kinetic Gas Theories and Multiparameter Correlation for Prediction of Dilute Gas Viscosity and Thermal Conductivity. *Industrial & Engineering Chemistry Fundamentals* **1984**, *23* (1), 8–13. https://doi.org/10.1021/i100013a002.

(305) Teja, A. S.; Rice, P. A Generalized Corresponding States Method for the Prediction of the Thermal Conductivity of Liquids and Liquid Mixtures. *Chem Eng Sci* **1981**, *36* (2), 417–422. https://doi.org/10.1016/0009-2509(81)85023-3.

(306) Ely, J. F. An Enskog Correction for Size and Mass Difference Effects in Mixture Viscosity Prediction. *Journal of Research of the National Bureau of Standards (United States)* **1981**, *86* (6), 597–604. https://doi.org/10.6028/jres.086.028.

(307) Brokaw, R. S. Approximate Formulas for the Viscosity and Thermal Conductivity of Gas Mixtures. II. *J Chem Phys* **1965**, *42* (4), 1140–1146. https://doi.org/10.1063/1.1696093.

(308) McAllister, R. A. The Viscosity of Liquid Mixtures. *AIChE Journal* **1960**, *6* (3), 427–431. https://doi.org/10.1002/aic.690060316.

(309) Wilke, C. R. A Viscosity Equation for Gas Mixtures. *J Chem Phys* **1950**, *18* (4), 517–519. https://doi.org/10.1063/1.1747673.

(310) Davidson, T. A. *Report of Investigations 9456 - A Simple and Accurate Method for Calculatlng Viscosity of Gaseous Mixtures*; 1993.

(311) Fuller, E. N.; Schettler, P. D.; Giddings, J. Calvin. New Method for Prediction of Binary Gas-Phase Diffusion Coefficients. *Ind Eng Chem* **1966**, *58* (5), 18–27. https://doi.org/10.1021/ie50677a007.

(312) Rackett, H. G. Equation of State for Saturated Liquids. *J Chem Eng Data* **1970**, *15* (4), 514–517. https://doi.org/10.1021/je60047a012.